



Norwegian University of  
Science and Technology

# Modeling and Experiments for Active Vapor Split Control of a Four-product Kaibel Column

**Johana Korbelaarova**

Chemical Engineering

Submission date: July 2018

Supervisor: Ivar Halvorsen, IKP

Co-supervisor: Sigurd Skogestad, IKP

Norwegian University of Science and Technology  
Department of Chemical Engineering



## Preface

This report is a master's thesis, which finalizes my studies for an international master's degree in Chemical Engineering at Norwegian University of Science and Technology (NTNU). This project work was carried out during the spring semester 2018 at the Department of Chemical Engineering, NTNU.

I would like to thank my supervisor Ivar Halvorsen for his help and patience with which he helped me. I appreciate his support and motivation during the semester, as we struggled with practical issues connected with the operation of the Kaibel column. Thanks go to Sigurd Skogestad as well for his time and technical knowledge he provided during consultations.

Trondheim, 2018

Johana Korbelarova

## Executive Summary

Kaibel column is studied as an energy efficient way of distillation. Kaibel column and other thermally coupled arrangements are introduced in theoretical part with focus on different approaches to control of these columns. The active vapor split as a controlled variable is reviewed.

The pressure drop evolution in Kaibel column is studied to understand its dependency on column variables. The known approaches for estimation of pressure drop are summarized in theoretical part.

The pressure drop in Kaibel column is studied experimentally. The pressure drop is strongly dependent on energy input. The total pressure drop increases, if one of the branches is closed, and the magnitude depends on amount of packing. The composition is also important factor for pressure drop, the feed with higher molecular weight, the pressure drop is higher. The change of liquid split does not have particular influence on pressure drop.

The model for pressure drop estimation in Kaibel column is created. The model is able to compute steady state values for total pressure drop, pressure drop in prefractionator, and main column, and vapor flows into respective branches. The input variables are reboiler duty, vapor split and temperature and composition in reboiler. The simulations show similar dependency on reboiler duty and vapor split as seen during experiments.

Experimental verification of different control structures for Kaibel column is reported. Product valves of distillate, and both side streams were used as manipulated variables together with liquid split, resp. vapor split.

The four-point temperature control of Kaibel column is studied. Control structure with liquid split control can reject feed disturbances, and setpoint changes of all variables.

For active vapor split control, the sensitivity of controlled temperature is strongly dependent on the position of the step change in manipulated variable. The system was able to reject setpoint change, liquid split disturbance and setpoint change of side stream control loop temperature.

The five-point temperature control of Kaibel column was introduced. The addition of second control loop to the prefractionator enables both liquid and vapor split control. The open loop experiments show incoherent responses for temperatures in top part of prefractionator. The strong dependency on control loop S1 was found. The sensitivity towards the liquid split is also rather low.

# Contents

Preface . . . . .	i
Executive Summary . . . . .	ii
<b>1 Introduction</b>	<b>3</b>
1.1 Motivation . . . . .	3
1.2 Related work . . . . .	4
1.3 Project objectives . . . . .	4
1.4 Outline . . . . .	4
1.5 Source Code . . . . .	5
<b>2 Kaibel Distillation Column</b>	<b>7</b>
2.1 Kaibel Distillation Column . . . . .	7
2.2 Control of Kaibel Column . . . . .	8
2.3 Devices for Active Vapor Split Control . . . . .	11
2.4 Pressure drop . . . . .	11
2.4.1 Modeling of the Pressure Drop in Experimental Kaibel Column	13
2.4.2 Experimental Estimation of Pressure Drop . . . . .	14
<b>3 Experimental Setup</b>	<b>17</b>
3.1 Kaibel Column . . . . .	17
3.2 Control Structure . . . . .	22
3.2.1 Parameters of the controllers . . . . .	23
3.2.2 Vapor Split Control . . . . .	24
3.3 Pressure Measurement . . . . .	25
<b>4 Pressure Drop Model for Kaibel Column</b>	<b>27</b>
4.0.1 Model Description . . . . .	27
4.0.2 Model Structure . . . . .	31

<b>5</b>	<b>Results</b>	<b>33</b>
5.1	Pressure Drop Experiments . . . . .	33
5.1.1	Change in Energy Input . . . . .	33
5.1.2	Change from Whole Column to Prefractionator and Main Column . . . . .	40
5.1.3	Liquid Split . . . . .	42
5.1.4	Heat-up . . . . .	43
5.2	Control Experiments . . . . .	46
5.2.1	Liquid Split Control . . . . .	46
5.2.2	Vapor Split Control . . . . .	51
5.2.3	5-point Temperature Control . . . . .	59
5.2.4	Pressure Drop Modeling . . . . .	62
<b>6</b>	<b>Conclusions</b>	<b>65</b>
6.1	Discussion . . . . .	65
6.2	Conclusions . . . . .	67
6.3	Recommendations for Further Work . . . . .	68
<b>A</b>	<b>Acronyms and Abbreviations</b>	<b>69</b>
	<b>Bibliography</b>	<b>70</b>



# Chapter 1

## Introduction

### 1.1 Motivation

Distillation process is a preferred solution for separation of liquid mixtures in industry, for example in oil refineries. Distillation itself has high energy demand, and it is desirable to minimize necessary energy input.

The motivation for reduction of energy consumption lies not only in economical reasons, but as well in environmental ones. Mainly, the lower energy consumption would cause higher reduction of emissions from energy production.

The one of possible solution how to reduce energy input is usage of Kaibel column, which was discovered by [Kaibel \(1987\)](#). Kaibel column is a type of dividing wall columns and enables separation of 4 components in one column. This oneshell arrangement of the thermally coupled distillation column has potential not only in energy savings, but as well in capital savings. In comparison to conventional sequence of binary distillation columns the energy savings can arise to 30%, as it was shown by [Halvorsen and Skogestad \(2006\)](#). The challenge lies in optimal operation of the column, because all possible energy savings could be lost by operating out of optimum.

The possibilities to enable optimal operation are researched, such as new control structures. The usage of vapor split as a manipulated variable was already introduced by [Strandberg \(2011\)](#). The experiments for vapor split control in this work build up on work published in doctoral theses of [Dwivedi \(2013\)](#) and [Strandberg \(2011\)](#).

As the vapor flow is strongly connected to pressure drop in the column, the pressure in Kaibel column is the other part of focus. The experiments were performed to capture the behavior, and the results were used to model of the pressure

drop for pilot plant Kaibel column.

The part of motivation for deeper study of pressure evolution was the pressure build up phenomena, which occurred during the previous project of mine, as this was widely discussed in the report [Korbelarova \(2017\)](#), although not being satisfactory explained. It was sought to reason this phenomena of pressure build up and pulsating in the column.

## 1.2 Related work

Part of scope of this thesis lies in study of active vapor split as a manipulated variable, the list of related works follows: [Strandberg \(2011\)](#) - Doctoral thesis focus on optimal operation of Kaibel distillation column and similar arrangements. [Dwivedi \(2013\)](#) - Doctoral thesis contains simulation and experimental studies of active vapor split control for different dividing wall column arrangements. [Kvernland \(2009\)](#) - Thesis introduces the model predictive control for Kaibel columns. [Korbelarova \(2017\)](#) - Project work of mine which focus on practical operation of laboratory Kaibel column. The other part of the scope lies in discussion of the pressure phenomena connected to operation of Kaibel columns. The background information about distillation columns, their design and pressure prediction comes mainly from: [Kister \(1992\)](#) [Maćkowiak and Maćkowiak \(2014\)](#)

## 1.3 Project objectives

The main objectives of this Master's project are:

1. Conduct experiments on laboratory Kaibel column with active vapor-split control
2. Introduce 5-point temperature control for Kaibel column
3. Conduct experiments on Kaibel column to study pressure drop dependency on input parameters
4. Create the pressure drop model of Kaibel column

## 1.4 Outline

Thesis is divided into theoretical, experimental and modeling parts.

- Chapter 2 focus on theory. First part summarizes published works about Kaibel column and other distillation columns with focus on control structures, and active vapor split. The other part of the chapter introduce ways for pressure drop estimation for packed distillation columns, and the approach, which was chosen for modeling.
- Chapter 3 shows the experimental setup of laboratory Kaibel column.
- Chapter 4 describes the pressure drop model of Kaibel column, its structure
- Chapter 5 summarize the results. First part is denoted to pressure drop experiments, the changes in reboiler duty, vapor split valve position, and liquid split are introduced to the system. The second part shows control experiments, studied controller structures were: 4-point temperature control using liquid split, 4-point temperature control using vapor split, and 5-point temperature control using both liquid and vapor split as manipulated variables. Final part shows results obtained by simulations.
- Chapter 6 contains discussion, conclusion and recommendations for further work

## 1.5 Source Code

The attached ZIP file contains source code for pressure drop model of Kaibel column.



## Chapter 2

# Kaibel Distillation Column

### 2.1 Kaibel Distillation Column

The Kaibel column was introduced by [Kaibel \(1987\)](#). The described column was able to separate four-component mixture into pure compounds in one column.

The Kaibel column is a type of dividing wall column (DWC), i.e. the part of column is separated by vertical partitioning wall. The dividing wall columns were known since 1930s ([Monro \(1938\)](#), [Wright \(1949\)](#), [Giroux \(1980\)](#)), but the industrial applications started in the middle of 1980s, around the time of introduction of Kaibel column.

The schematic of Kaibel column is in figure [2.1](#). The 4-component feed mixture enters the left branch of the column, which is called prefractionator. In prefractionator, the separation between lighter and heavier components occurs. In the right branch, or in other term in main column, the separation is finished and the products are drained. The energy input is provided by reboiler in the bottom of the column, where heaviest product D is obtained. The streams for the side products B and C withdrawal are situated along the main column. The top of the column is equipped with total condenser, where the vapor flow is condensed into liquid, part of the liquid is leaving the column as the lightest product A.

Kaibel column is able to replace conventional setup of three binary distillations columns (see figure [2.2](#)). The energy savings while using the Kaibel column, can arise to 30%, as it was shown by [Halvorsen and Skogestad \(2006\)](#). The second savings lies in lower capital costs, and the one-shell arrangement also occupies less space.

The Kaibel column is thermally equivalent to Petlyuk arrangement for four components. [F. B. Petlyuk \(1965\)](#) introduced the three-compound thermally cou-

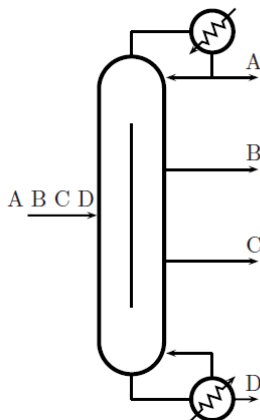


Figure 2.1: Kaibel column, 4-product dividing wall column, [Strandberg \(2011\)](#)

pled distillation column, which enabled separation of the products with significant energy savings compare to conventional series of distillation columns. Petlyuk modified the three-compound arrangement for four-component separation. Both Petlyuk arrangements are shown in figure 2.3.

To illustrate the industrial applications of Kaibel columns and other dividing wall column setups, data presented by [Olujic \(2016\)](#) at EFCE WP Fluid Separations 2016 are presented. Since the first DWC column was put in operation by BASF in 1985, and the industrial Kaibel column was introduced (see [Olujic et al. \(2009\)](#)), more than 250 dividing wall columns were put in operation. More than 90% of DWCs are equipped with packed beds, the rest consist of the tray dividing wall columns, where the former ones are in use since 2000. The new multipurpose DWC column was put in operation in 2010, this column enables batch distillation, side product column and conventional two column sequence in one column.

## 2.2 Control of Kaibel Column

The control of Kaibel column, and other dividing wall columns was deemed challenging. One of the first control studies was published by [Wolff and Skogestad \(1995\)](#), the control of Petlyuk column was achieved by three-point composition control, and liquid split was proposed as a controlled variable.

It was found by [Strandberg and Skogestad \(2006\)](#), that the four-point temperature control with inventory control can stabilize Kaibel column and prevent "composition drift". This was verified by conducting experiments on laboratory

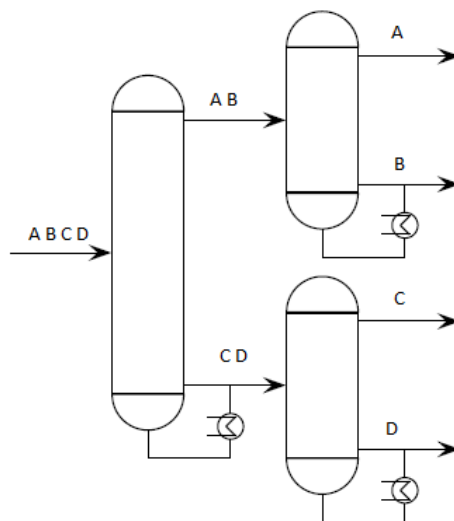


Figure 2.2: Conventional setup of 3 binary distillation columns for separation of 4-component mixture, [Kvernlund \(2009\)](#)

Kaibel column, as reported in doctoral theses of [Strandberg \(2011\)](#), and [Dwivedi \(2013\)](#).

Similarly, [Qian et al. \(2016\)](#) recently reported simulation results for temperature control of three product DWC. Among others, three-point temperature control structures were tested with liquid split, or vapor split, as manipulated variables. The study confirms the previously reported results.

The optimal operation of three-product Petlyuk column was studied by [Halvorsen and Skogestad \(1999\)](#). There is a rather narrow window, where it is possible to achieve operation optimum. The liquid split and vapor split were related to boilup in this study.

The results were confirmed by [Dwivedi \(2013\)](#) in his doctoral thesis (chapter 5) where the simulation was broadened to four-product Kaibel column. It is shown that close relation between energy usage (given by boilup) and vapor split exists. If the vapor split shifts out of optimum due to disturbance, the energy usage increases. The active control of vapor split enables to avoid this situation.

Previously mentioned doctoral thesis by [Dwivedi \(2013\)](#), is a comprehensive study on usage of active vapor split for different dividing wall columns and Petlyuk columns. Part of the results are confirmed experimentally.

[Kvernlund et al. \(2010\)](#) studied the multivariable Model Predictive Controller with a four-point temperature control for Kaibel column. The model can be fitted

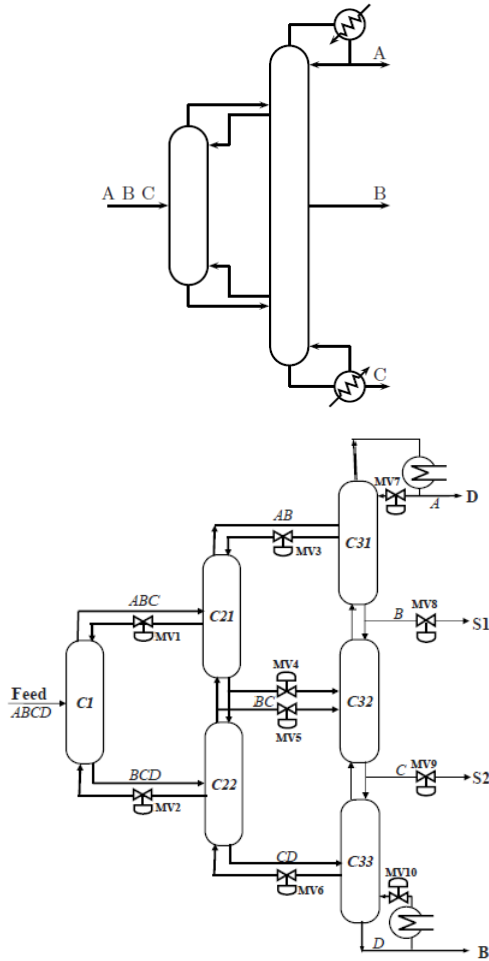


Figure 2.3:

Top: Petlyuk arrangement for separation of 3-component mixture, [Strandberg \(2011\)](#)

Bottom: Petlyuk arrangement for separation of 4-component mixture, [Dwivedi \(2013\)](#)

to laboratory Kaibel column at NTNU, and the MPC control added into Labview interface as Kvernland proposed in his diploma thesis later (Kvernland (2009)).

Yet another control structure was proposed by Dwivedi et al. (2012) on 2<sup>nd</sup> Trondheim Gas Technology Conference. The 5-point temperature control structure adds second controlled temperature in prefractionator to enhance the controllability of prefractionator. The structure is similar to 4-point control, but temperatures in prefractionator are controlled by adjustment of both, the vapor and the liquid split. This approach, which yet has to be verified, is further studied in this thesis.

## 2.3 Devices for Active Vapor Split Control

Different approaches for realization of active vapor split are researched, and some of them are even patented.

Active vapor split device was realized on laboratory Kaibel column at NTNU developed by Strandberg (2011). Two separate vapor valves in each column branch are operated by external stepper motors. The rack and pinion assembly is used, and vapor flow is adjusted by changing the cap position. Vapor split valves are described in more detail in Experimental Setup section, see figures 3.4 and 3.5 showing pictures, and schematic of the vapor valves.

In 2014, King and Haas patented an external vapor control system, The vapor flow is lead outside of the column and again redistributed to individual sections.

Experimental study by Ge et al. (2014) presents vapor split control by changing of the angle of the blades on special tray. These blades are connected to axles operated by external electrical motors. The implemented tray consist of adjustable blades, vapor distribution plate, V shaped cups, and liquid downcomer. In 2017, Joon Kang et al. (2017) introduced hydraulic driven active vapor split distributor which lacks mechanical motor and other moving parts. Modified chimney tray with special cups is added to both sections with the adjustable liquid level in each section. And finally he vapor flow is manipulated by level controller, which is adjusting the ratio between the liquid levels on the tray.

## 2.4 Pressure drop

The pressure drop is important parameter for column design and operation. The pressure drop values and the approach for its estimation depends on the packing type. This statements applies to the tray distillation columns as well, for example, the pressure drop for sieve and valve trays calculations differ, but since the main

focus lays due to experimental setup in the packing type columns, the tray columns would not be further discussed.

The pressure drop is given by packing type, vapor flow, liquid load, and column height, and diameter.

The total pressure drop for packing height  $\Delta p/\Delta z$  consists of pressure drop given by dry packing  $\Delta p_0/\Delta z$  and the liquid hold up quotient  $\Delta p/\Delta p_0$ , which denotes the influence of liquid holdup on pressure drop. As stated in equation 2.1 by Mackowiak (2010):

$$\frac{\Delta p}{\Delta z} = \frac{\Delta p_0}{\Delta z} \frac{\Delta p}{\Delta p_0} [\text{Pa/m}] \quad (2.1)$$

The dry pressure drop estimation is important for estimation of gas velocity flooding, and of the lower limit of operation range.

The irrigated pressure drop estimation is used for flooding prediction, pressure drop estimation for whole range of liquid loads up to the flooding point.

For decades, the pressure drop and flooding points were estimated using Sherwood-Eckert generalized pressure drop correlations (GDPR) chart. First this chart, introduced by Sherwood et al. (1938) and modified by Lobo et al. (1945) contained line of flooding points only. It was extended by Leva (1954), who added pressure drop curves below the flooding for different packing. Further modifications were added by Eckert (1975). Strigle (1994) modified the logarithmic scale to semilogarithmic, which is the most current and used version. Furthermore, the diagram for random packing was modified for structural packing by Kister and Gill (1992), who introduced the generalized diagram for structural packing. The recent paper by Kister et al. (2007) denotes the nowadays usage, and dos and dont's in interpolations, and correlations of GDPR.

The GDPR approach has its concurrence and buildup in the modeling and computer modeling. The models for random packing for irrigated pressure drop were published by authors like Stichlmair et al. (1989), Kister (1992), Billet and Schultes (1991), Billet (1995), Maćkowiak (1991), the complete list of their work up to 2014 was summarized in Maćkowiak and Maćkowiak (2014).

The structured packing models were reported by Rocha et al. (1993), Olujić (1997), Shilkin and Kenig (2005), E. Brunazzin (1997), Stichlmair et al. (1989).

The software tools for prediction of hydraulic performance were developed by commercial companies for their products. The first one was introduced by Sulzer in 1998 named Sulpak and later renamed to Sulcol. TM Similar programs were introduced; KG-TowerTM by Koch-Glitsch, Winsorp by Raschig, Rapsody by RTV, Trayheart by WelChem, and Device Rating Program by DRP. AspenPlus, Hysis, or other commercial process simulation programs provide built in hydraulic corre-

lations from the vendors mentioned above.

The biggest resistance of the vapor flow is caused by column packing. Although, some of the column internals can cause the restriction to the vapor flow especially for low pressures, as it was shown by [Rix and Olujic \(2008\)](#). The article studies the pressure drops caused by liquid collectors and distributors.

From practical point of view, the properties of particular packing need to be established. These studies are using water-air mixture or other standard mixtures (nonpolar ones) to find packing parameters. These parameters are then base for calculations and modeling.

### 2.4.1 Modeling of the Pressure Drop in Experimental Kaibel Column

The modeling of laboratory Kaibel column is complicated due to its experimental setup. Packing in the column consist of glass Raschig rings with 6 mm in diameter, and pieces of structural packing, which keeps the Raschig rings at given column sections.

The well established models for random packing, like [Billet \(1995\)](#), are designed for industrial applications, and lack the values for Raschig rings of this size and material.

The structural packing models generally use geometry of the packing and other parameters for pressure drop estimation.

The precise approach would require to combine models for structural and random packing, and internals. This could be complex procedure to calculate though due to measurement and its accuracy it's not necessary overall as empirical approach is preferred.

The empirical approach was adopted due to unusual experimental setup. Following equation 2.2 estimates pressure drop per packing bed height  $\Delta p/\Delta z [Pa/m]$ . The equation is from Sulcol software package for columns with internal diameters larger than one meter, also mentioned by [Duss \(2013\)](#). Although, since the laboratory column has diameter considerably smaller than one meter, the equation was primarily used for modeling purposes.

$$\frac{\Delta p}{\Delta z} = \frac{c_f}{d_h G} \frac{\rho_G u_{Gs}^2}{2} \quad (2.2)$$

where  $\Delta z[m]$  is packed bed height,  $c_f[-]$  represents drag coefficient,  $\rho_G[kg/m^3]$  is vapor density,  $u_{Gs}[m^3/m^2s]$  is superficial gas velocity. The hydraulic diameter of gas flow channel  $d_h G[m]$  depends on specific geometric area of packing  $a_p[m^3/m^2]$ ,

see equation 2.3.

$$d_h G = 4a_p \quad (2.3)$$

First, experiments were conducted to establish the drag coefficient of the packing. The pressure drop was measured for different vapor flows in operating range, and the drag coefficient was calculated from these values. The actual pressure drop is then calculated using known resistance per packing multiplied by height of the packing.

## 2.4.2 Experimental Estimation of Pressure Drop

The pressure drop for realized columns can be estimated by experimental measurement, by pressure sensors with requisite precision and range installed alongside the column. In industry, this measurement usually serves not only as a measurement, but as well as a safety feature. The large increase of the pressure can indicate the unstable operation state, such as lack of liquid in the reboiler. The safety procedures are usually connected to the measurements, and shut-down procedure can start automatically at the moment the unstable operation is indicated by pressure, or other measurement.

For small pressure drops, the other possibility for estimation of the pressure drop is to use U-tubes filled with liquid, which ends are connected to the measurement points. The measurement is based on hydrostatics in gravitation field, on the principle of the Pascal's law. The hydrostatic pressure is estimated by equation 2.4, where the pressure drop  $\Delta p$ , is calculated from the level difference  $\Delta h$ , gravitaional force  $g$ , and density of the liquid in U tube  $\rho$ .

$$\Delta p = \Delta h \rho g \quad (2.4)$$

The experimental Kaibel column operates at the normal pressure, as the column is open to the atmosphere on the top. The pressure measurements are realized as U tubes with one end connected to the column and the other end open to the atmosphere. The measured values indicates the pressure drop between point of the measurement and the top of the column. The measurement points were mainly chosen based on practicality of the realization, the list of measurement points follows:

- Reboiler – measurement of total pressure drop
- Vapor split valves – measurement of pressure bellow and above the vapor

split valves in prefractionator and main column (indicated as PA, PB, MA, MB)

- Feed – measurement by feed entrance in prefractionator
- S1 – measurement by side stream 1 in main column
- S2 – measurement by side stream 2 in main column



# Chapter 3

## Experimental Setup

This chapter explains the setup of the experimental column at Department of Chemical Engineering, NTNU. The description of the experimental setup is based on previously conducted experiments and my previous project work, which the thesis is a continuation of.

### 3.1 Kaibel Column

The experimental column situated in laboratory Hall C at the Chemical Engineering Department, NTNU is shown in figure 3.1, (Strandberg, 2011). Kaibel column is realized as a two-shell, although this geometry is thermodynamically equivalent to dividing wall column. This column was built by Strandberg (2011) during his Ph.D. studies at NTNU, more detail information about column could be found there.

The column is made of glass sections produced by Normag Labortechnik in Germany. The individual sections are connected by flanges. Flanges are attached to aluminum frame by springs, which lowers the pressure on sections below, and secures column position.

As seen in the figure 3.1 (Dwivedi, 2013), the column consists of 7 sections, sections 1 and 2 (left branch) represents prefractionator, while 3 to 7 represent the main column. The sections are vacuum coated, and covered by silver to minimize heat loss. The inner diameters of the sections are written in table 3.1.

Column is packed by glass Raschig rings with diameter of 6 mm. The packing high varies in column sections; the values are summarized in table 3.1. The height equivalent of a theoretical plate (HETP) was estimated by Dwivedi (2013) to be 16 cm for this column.

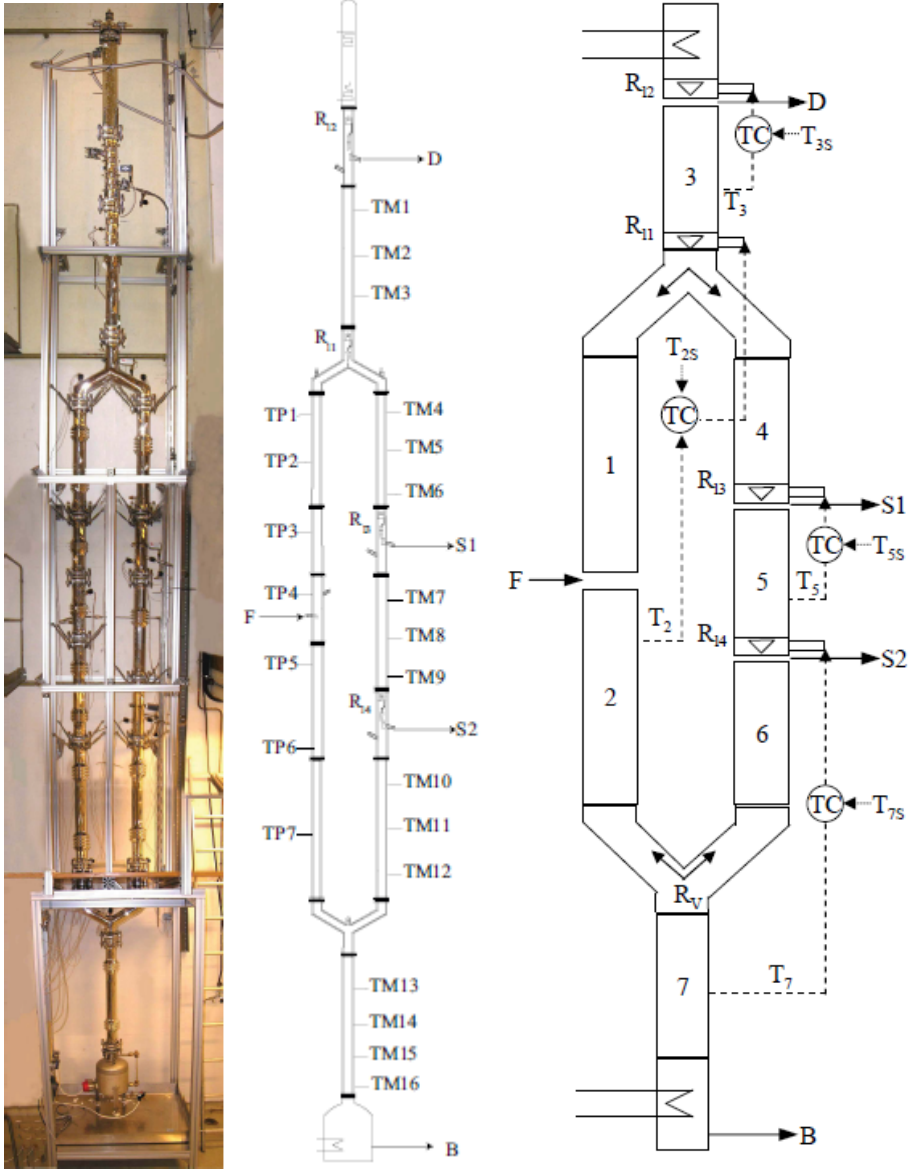


Figure 3.1: Picture and schematics of experimental Kaibel column, Dwivedi (2013), from left to right:

Picture of experimental column

Schematic of location of temperature sensors

Schematic of the column sections, with liquid split control structure

Section	Inner diameter [mm]	Packing height [m]
1	50	1.10
2	50	1.60
3	70	0.65
4	50	0.65
5	50	0.65
6	50	0.75
7	50	0.90

Table 3.1: Specification of column sections



Figure 3.2: Picture of side stream product withdrawal. Swinging funnel leads the liquid from collector outside the column as a product, or back as a reflux.

The valves ensuring the liquid split and product withdrawal are swinging funnels operating at ON/OFF states controlled by externally placed solenoids. The positions of funnel are changing with given period to ensure preferred liquid split, and stable liquid flow in the column.

The side stream withdrawal is shown on figure 3.2, the swinging funnel inside directs the liquid flow outside the column as a product, or back as a reflux.

The liquid split section is shown on schematic, figure 3.3, liquid is accumulated in collector, the funnel directs the liquid flow according to solenoid either to prefractionator on the left, or to main column on the right.

This column enables usage of vapor split as a manipulated variable. This is facilitated by two vapor split valves developed by Strandberg (2011), see figure 3.4.

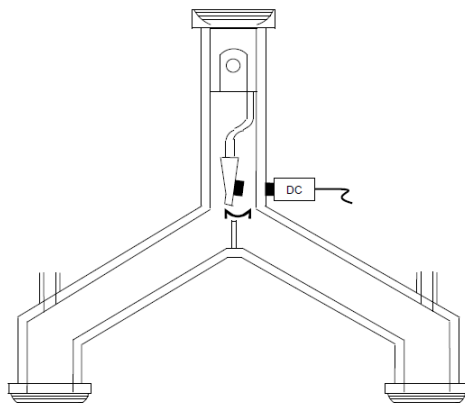


Figure 3.3: Schematic of liquid split. Swinging funnel leads liquid flow according to solenoid to prefractionator (left), or to main column (right).

Valves are operated by external electrical motors.

The schematic of vapor split valve is presented in figure 3.5. The rack and pinion assembly is used, the vapor flow is adjusted by changing the cap position, the liquid downcomer allows liquid to flow against vapor. Two valves are situated in lower parts of section 2 and 6 in prefractionator, and main column, respectively.

The side stream coolers are installed to lower the temperature of leaving product. The liquid seal on product stream, following coolers, avoids the leakage of vapor through side stream, which would cause disturbance to the process. This also work as indicators of pressure drop in respective column section. See figure 3.7.

The reboiler is kettle type electric boiler with maximal energy input 2.9 kWh. Energy input is adjusted by thyristor. Reboiler capacity is 15 l, while operation minimum is 3 l. Since the level control on reboiler is not implemented, the bottom product is kept accumulating in reboiler during experiments.

The top of the column is equipped by condenser cooled by water. The condensed product liquid flows back to column to split valve where is divided to distillate and liquid reflux.

The feed is pumped into the system by a digital diaphragm dosing pump. Possible flow range is 0.2-20 l/h. The electric heater is installed alongside the feed tube to preheat feed, and lower the disturbance caused by cold liquid entering the column.

The column is operated at atmospheric pressure, the total pressure drop under normal operation is about 0.016 bar.



Figure 3.4: Picture of vapor split valve.

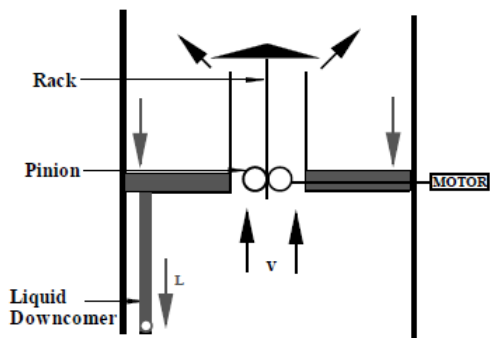


Figure 3.5: Schematic of vapor split valve. The vapor flow is changed by adjusting cap position through rack and pinion by electric motor.

The separation of equimolar mixture of primary alcohols is studied. The feed mixture consist of methanol, ethanol, 1-propanol and 1-butanol.

## 3.2 Control Structure

The decentralized control structure is implemented in the LabView control interface. The control layer can consist of up to five feedback control loops. The temperature measurements among the column were used as controlled variables.

As it was published by [Strandberg \(2011\)](#), the 4-point temperature control is enough to ensure stable operation of 4-compound distillation columns, and avoiding the 'drift' of product composition.

The manipulated variables were chosen from degrees of freedom of this column. Feed rate and feed composition, and the energy input were kept constant unless used as disturbances. The remaining manipulated variables were used for control purposes, these are summarized in the following list:

- Liquid split valve RL, ratio between liquid flow to prefractionator and total flow from top section:

$$RL = \frac{L_1}{L_3} \quad (3.1)$$

- Vapor split valve RV, ratio between vapor flow to prefractionator and total flow from reboiler:

$$RV = \frac{V_2}{V_7} \quad (3.2)$$

- Distillate product split valve RD, ratio between liquid flow from top section and total liquid flow of condensate:

$$RD = \frac{L_3}{L_3 + D} \quad (3.3)$$

- Side stream 1 product split valve RS1, ratio between liquid flow below the side stream 1 and liquid flow above side stream 1:

$$RS1 = \frac{L_5}{L_5 + S1} \quad (3.4)$$

- Side stream 2 product split valve RS2, ratio between liquid flow below the side stream 2 and liquid flow above side stream 2:

$$RS2 = \frac{L_6}{L_6 + S2} \quad (3.5)$$

Loop name	Manipulated variable	Controlled variable
Control loops present in all structures:		
D control loop	RD	TM3(T2)
S1 control loop	RS1	TM8 (T9)
S2 control loop	RS2	TM14 (T13)
Control Structure 1: liquid split		
+RL control loop	RL	TP5(TP5)
Control Structure 2: vapor split		
+RV control loop1	RV	TP7(TP7)
Control Structure 3: vapor and liquid splits		
+RL control loop	RL	TP1(TP1)
+RV control loop1	RV	TP7(TP7)

Table 3.2: Feedback control loops and control structures.

where L, and V refers to liquid, resp. vapor flows in individual sections as defined in figure 3.1.

Different control structures were used during experimental work. The control loops used during experimental work are summarized in table 3.2. The product control loops - D, S1 and S2, were used in combination with liquid split, vapor split, or both. The controlled temperatures were chosen primarily according to sensitivity towards respective manipulated variables, and secondarily to avoid the interactions between control loops. The interactions were mainly discussed for proposed control structure 3 from table 3.2.

There is one extra feedback control loop, which is not mentioned in table 3.2. The feed is heated before enters the column, this controller regulates temperature of heating element.

### 3.2.1 Parameters of the controllers

Some of the controller parameters, and other settings are known from previous experiments and were presented by korb REF. The following table 3.3 summarizes these results. The  $X$  denotes part of the parameters for RL and RV control loops. The setpoint temperatures for prefractionator are not denoted because this temperature is strongly dependent on feed composition. The controller parameters for RV and RL control loops are skipped as these are part of project work and different approaches are presented in the Result section.

Name	MV	Min - Max	Kp	I	CV	Setpoint [°C]
D loop	RD	0 - 1	-0.3	4	TM3(T2)	70
RL loop	RL	0.3 - 0.7	-0.03	4	TP5(TP5)	X
or RL loop 2	RL	0.3 - 0.7	X	X	TP1(TP1)	X
RV loop	RV	0.1 - 0.9	X	X	TP7(TP7)	X
S1 loop	RS1	0 - 1	-0.18	4	TM8(T9)	90
S2 loop	RS2	0 - 1	-0.32	4.16	TM14(T13)	112
Feed flow	-	0 - 10	0.65 -	-	-	-
Reboiler	-	0 - 2	-	-	-	-
Feed Heater	heat input	1 - 0	-0.03	10	Feedheat1	30-60

Table 3.3: Settings for Kaibel column: Limit values and PI Controller settings.

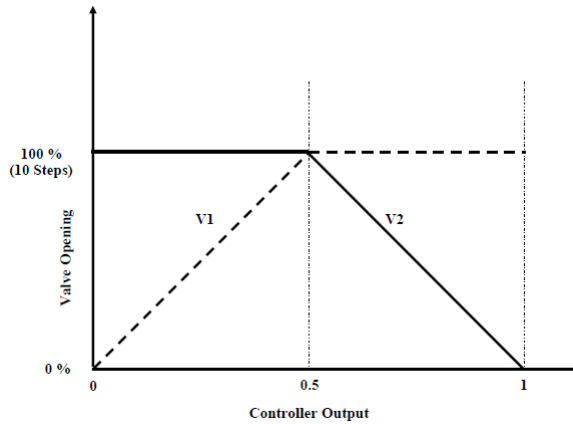


Figure 3.6: Vapor split RV controller - split range control.

### 3.2.2 Vapor Split Control

The vapor valves were described in previous section in general. The valves has 150 steps to operate on, but as it was shown by Dwivedi (2013), only the first 8 steps are actually influencing the vapor flow. The regulation of vapor flow is desired through increasing of the resistance for vapor flow by closing of the valves. The vapor split controller is operating as split range controller, where one half of the range is operated by vapor valve in prefractionator, and the second half is operated by vapor valve in main column branch. The schematic description is in figure 3.6 by Dwivedi (2013).

### 3.3 Pressure Measurement

Pressure is measured as difference of levels in U-tubes, where one end is connected to the column and the other is open to the atmosphere. The measured value, height of liquid column is easily transformed by formula for Pascal's to pressure difference between the column and atmosphere.

The positions of measurement U-tubes are situated by reboiler, on feed, on product side streams S1 and S2, and on vapor split valves - above and below each of them. Pictures of exemplar measurement sites, reboiler and side stream S2 are presented in figure 3.7.

The reboiler measurement site is screened by camera, which is connected to the PC on the first floor, and enables to capture a video. Videos of pressure changes were scattered into pictures, where one picture every 30 seconds was saved and analyzed for liquid column height using ImageJ software. The measurements of others sites were noted in real time with intervals ranging between five and seven minutes.

The pressure measurements for distillation column were performed during total reflux experiments, where no feed was introduced to the column, no products were withdrawn, and control loops were turned off.

Part of the experiments were carried with all compounds of feed mixture, while the other ones were carried with butanol as the only compound to uncover the influence of composition, and temperature profile. Later, these groups would be referred to as pressure 4-compound experiments resp. pressure butanol experiments.



Figure 3.7: Picture of pressure measurements, reboiler and sidestream 2, which works as liquid seals too. It ensures that the vapor is not leaking through the tubes.

## Chapter 4

# Pressure Drop Model for Kaibel Column

Pressure drop model for Kaibel column is created in MATLAB. Model uses built-in solver for nonlinear systems `fsolve` to calculate steady state values of pressure drop, and vapor flows from initial conditions.

### 4.0.1 Model Description

Pressure drop model is based on relatively simple principle. The pressure drop is established as vapor flow from reboiler meets resistance of packing and other internal parts on its way to the top of the column.

This column resistance is divided into sections. Seven of these sections copy the sections of the packing. Two extra sections are formed by manipulated vapor split valves, which change the ratio of vapor flow into each section by increasing the flow resistance.

The figure shows the schematic of the model. Packing sections of the column are denoted by numbers 1-7.  $P_T$  is total pressure drop.  $P_P$  represents pressure in pre-fractionator, which consists of pressure drop caused by packing  $P_{P0}$ .and adjustable pressure drop caused by vapor valve  $P_{PV}$ . Similarly,  $P_M$  denotes pressure in main column, which consists of pressure drop caused by packing  $P_{M0}$ , and adjustable pressure drop caused by vapor valve  $P_{MV}$ .

The molar vapor flow from reboiler  $V_m$  splits into vapor flow in prefractionator  $V_P$  and main column  $V_M$ .

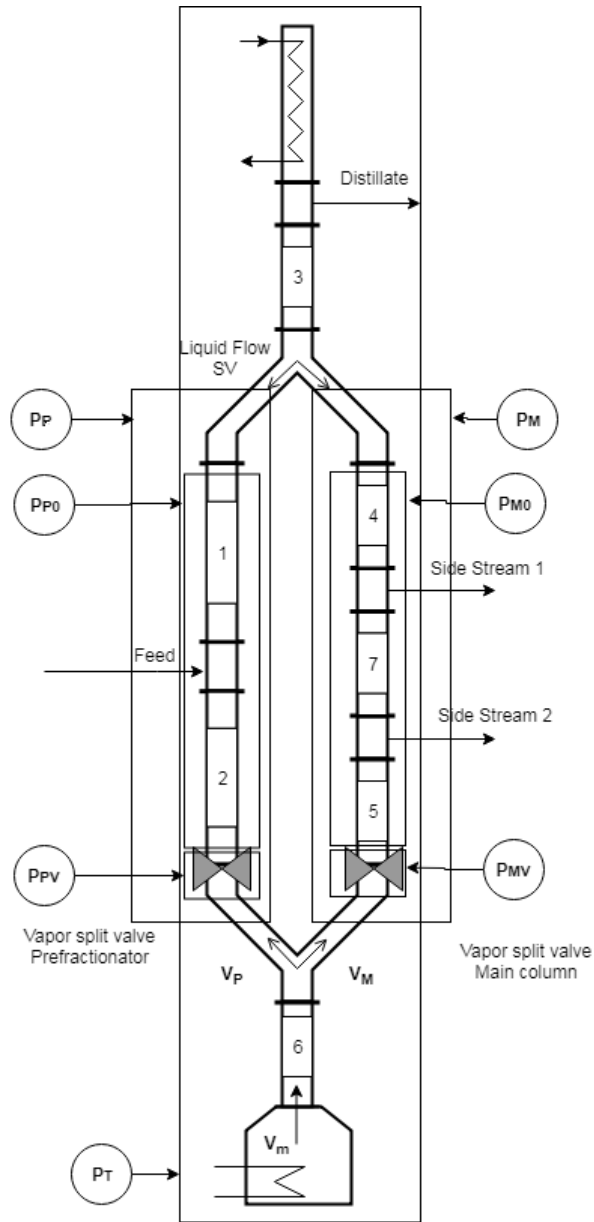


Figure 4.1: Schematic of pressure drop model

The equation for resistance of packing is derived from Sulcol equation.

$$\frac{\Delta p}{\Delta z} = c_f 4 a_p A M r_{mix} z_c R T b_{mix} p_a \quad (4.1)$$

where  $c_f[-]$  is drag coefficient given by experiments,  $a_p[m^3/m^2]$  specific geometric area of packing,  $A[m^2]$  column cross sectional area,  $M r_{mix}[g/mol]$  is molar weight of the mixture,  $T b_{mix}[K]$  is boiling point of the mixture  $R[J/molK]$  ideal gas constant,  $z_c$  is compressibility factor,  $p_a$  atmospheric pressure. The properties of gas mixture were based on average composition of each section.

With all constants multiplied by packing height we get the resistance of the packing, as in equation for pressure drop as a function of molar vapor flow and packing resistance:

$$\Delta p = R V_m^2 \quad (4.2)$$

The resistance of packing in column sections:

- $R_B$  bottom section
- $R_C$  top section
- $R_{P0}$  packing in prefractionator
- $R_{M0}$  packing in main column

Valve resistance  $R_{PV}$ ,  $R_{MV}$  is adjustable, given by parameter  $k$  and valve position  $z$  (0,8), which is calculated from RV:

$$R_{PV} = k_{PV}(z_{PV} - 8) \quad (4.3)$$

$$R_{MV} = k_{MV}(z_{MV} - 8) \quad (4.4)$$

Then, total resistance in prefractionator:

$$R_P = R_{P0} + R_{PV} \quad (4.5)$$

Then, total resistance in main column:

$$R_M = R_{M0} + R_{MV} \quad (4.6)$$

And finally total resistance in whole column, i.e. total resistance:

$$R_T = R_B + \frac{R_P + R_{P0}}{R_P + R_{P0} + R_M + R_{M0}} + R_C \quad (4.7)$$

### Model Equations

The system of nonlinear equation is given.

Total pressure drop equation:

$$\Delta p_T = R_T * V_m^2 \quad (4.8)$$

Vapor flow split equation:

$$V_m = V_P + V_M \quad (4.9)$$

At steady state, pressure drops for prefractionator and main column are equal:

$$\Delta p_P = \Delta p_M \quad (4.10)$$

Delta pressure in prefractionator and main column:

$$\Delta p_P = R_P * V_P^2 \quad (4.11)$$

$$\Delta p_M = R_M * V_M^2 \quad (4.12)$$

### Model Variables, Parameters and Initial values

Model inputs:

- Reboiler duty
- Vapor split
- Temperature in reboiler
- Composition in reboiler

Initial values:

- Vapor flow in prefractionator
- Vapor flow in main column
- Total pressure drop
- Pressure drop in prefractionator
- Pressure drop in main column

Parameters: Molar weights of alcohols; Liquid densities of alcohols; Boiling temperatures of alcohols; Packing height; Column diameter; Drag coefficient; Specific geometric area of packing; Coefficients for heat of vaporization; Average composition for each section; Ideal gas constant; Compressibility factor; Atmospheric pressure; Valve resistance;

## 4.0.2 Model Structure

Model consist of several connected MATLAB functions.

- `Kaibelpressure.m` – is the main file running the model, the input data and parameters are included
- `pressuremodel.m` – pressure drop model solved by `fsolve`
- `vaporenthalpy.m` – calculates heat of vaporization for given temperature, and mixture composition
- `reboilerduty.m` – fits reboiler duty settings to actual energy input, adds 10% heat loss
- `reboiler.m` – calculates molar vapor flow from energy input
- `drag_coeff.m` – calculates drag coefficient for column packing, separate file, not in model itself



# Chapter 5

## Results

### 5.1 Pressure Drop Experiments

Various experiments were conducted to examine the factors influencing the pressure drop. The experiments run at total reflux, with no feed entering and no product withdrawal, although some leaking through the product steams was observed, the phenomena is further analyzed in Discussion.

The examined factors were energy input (and consequently vapor flow), liquid split and vapor split through closing one of the branches. In addition, one extra factor was discovered after the first conducted experiments. The results for liquid split changes did not show any coherent effect, and seemed biased. It was assumed that the slow changes in composition (and temperature) could be the possible cause. Therefore, the butanol was used instead the feed mixture as the only chemical in the column.

Another circumstance occurred soon after the first experimental runs, it was found that the measuring points by vapor split valves PA, PB, MA and MB are not reliable. It was observed, that the vapor is condensing in narrow measuring tubes connecting the measuring hoses with split valves, the condensate is forming liquid plug, and results in decreasing of measured values. The valve measurements are omitted in presented results.

#### 5.1.1 Change in Energy Input

The change in energy input is reported for butanol, and four compound experiments. The pressure drop evolution is explained, together with changes in temperature profile.

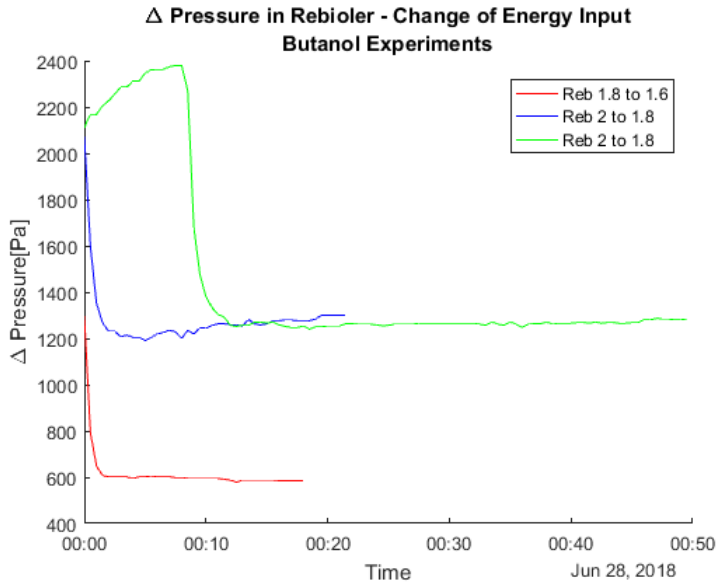


Figure 5.1: The pressure drop evolution in reboiler, change in reboiler duty, butanol experiment.

### Butanol Experiment

The total pressure difference in reboiler for whole column after step change of energy input (reboiler duty) is shown in figure 5.1. The plot summarizes data from several butanol experiments. The operation of column at reboiler duty  $Q = 2$  is not stable. The flooding was observed in upper section of the column (section above the connection of the two branches), this was indicated by sound of the Raschig rings flooding inside of the column section. This unstable operation is given due to difference in molecular weight of methanol and butanol, and therefore the difference in volumetric flow. This phenomena was already explained by [Strandberg \(2011\)](#), and it was the reason to enhance the column with wider 'Y' section in the bottom of the column.

For this reason, the step changes in reboiler duty from 2 to 1.8, the pressure difference was not stabilized at higher reboiler duty 2.

The green line shows the step changes in reboiler duty from 2 to 1.8, the pressure is stabilizing in the beginning, increasing from 2.1 to almost 2.4 kPa, then in eight minute from the beginning, the step change is introduced, and the pressure difference drops to 1.4 kPa in two minutes, and later stabilize at 1.26 kPa. The change in pressure drop would be around 1.1 kPa.

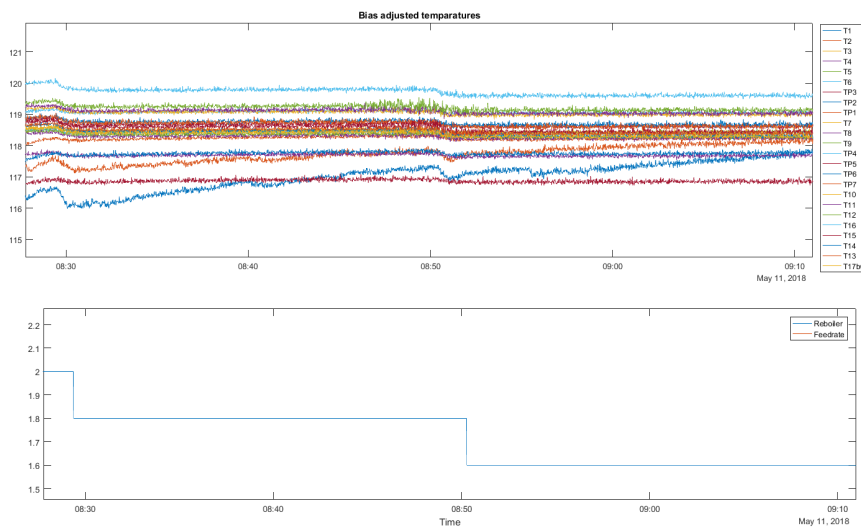


Figure 5.2: The temperature evolution, change in reboiler duty, butanol experiment.

The blue line indicates the same step change, but there the step had to be made before stabilizing pressure at reboiler duty 2 due to occurrence of flooding. The step change was introduced shortly after beginning of the measurement. The pressure change from nearly 2.1 kPa to 1.2 kPa in two minutes, later stabilizes in 20 minutes at 1.3 kPa. The change in pressure drop would be ca 0.9 kPa, which is lower compare the other experiment, but it has to be noted that the initial pressure was not stabilized, and probably would be higher.

The red line indicates change in reboiler duty from 1.8 to 1.6, the step change was done soon after beginning of the measurement. The first point indicates steady state pressure difference at reboiler duty 1.8, nearly 1.3 kPa, which drops in about two minutes to 0.6 kPa and stabilizes there. The net pressure drop after step change would be ca 0.7 kPa.

The changes in temperature profiles are visible on figure 5.2 for two step changes from previous figure (blue and red line). Temperature changes after these steps are relatively small. Its influence was observed for three the temperatures of all measured. The light blue temperature curve at 120°C denotes T16 temperature closest to the reboiler. This temperature drops around 0.2 °C after each step change. Whereas, the other temperatures are on the top of the column. Blue T1 and red T2, are the temperatures which are shifting the most, these temperatures drop down about 0.3-0.5°C before returning to the previous trend.

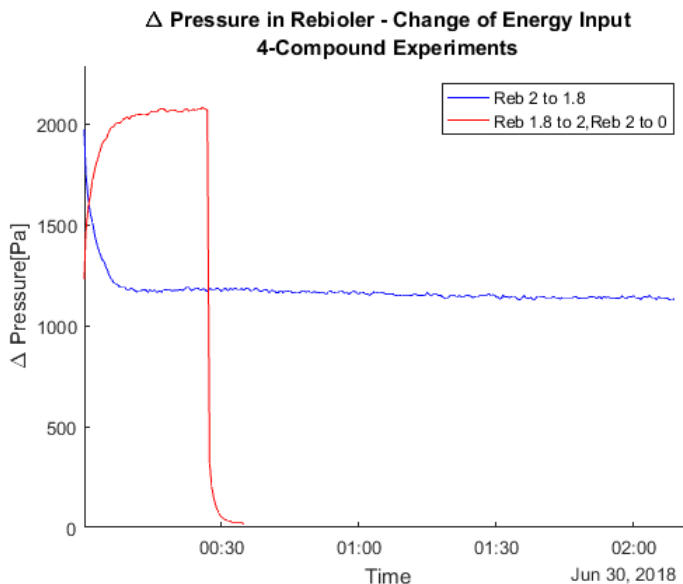


Figure 5.3: The pressure drop evolution, change in reboiler duty, 4-compound experiment.

It can be concluded that the changes in pressure drop in reboiler after inducing the change in reboiler duty are significant, because the energy input has direct impact on amount of evaporation heat, and directly influences vapor flow in the column. The temperature for butanol experiments is not influenced, the most significant change can be seen for the temperature in reboiler, and T1, and T2 temperatures on the top, which were stabilizing during conducted step changes.

#### 4-compound Experiment

The pressure evolution for 4-compound mixture after the change in reboiler duty is shown in figure 5.3.

The red line illustrates two changes of reboiler duty. First, the reboiler duty changes from 1.8 to 2, and the pressure drop increases from 1.25 kPa to 2.1 kPa in ca 10 minutes.

Later, the energy input is completely stopped, as during shutdown procedure. The pressure drops to 250 Pa immediately after the step, then the decrease slows down, and in three minutes the pressure drop is almost 0. The slowing of the response, is due to heat capacity of the reboiler, the heating element is still warm, and the reboiler contains ca 8 liters of liquid at temperature close to the boiling

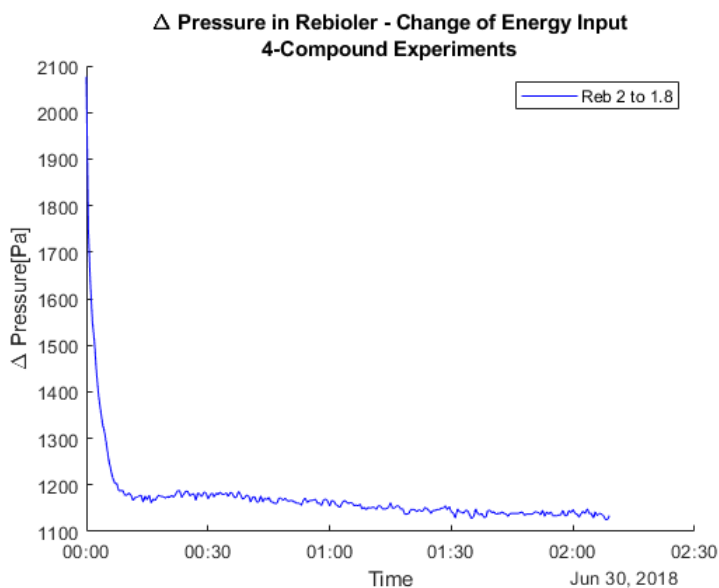


Figure 5.4: The pressure drop evolution, change in reboiler duty from 2 to 1.8, 4-compound experiment, capturing evolution in time.

point.

The blue line shows step change from 2 to 1.8, where the pressure drop changes from old steady state at 2.05 kPa, to new one at 1.2 kPa in 8 minutes.

In comparison to butanol experiments, the steady state pressures are lower for all 4 compounds present. For the same molar flow, the volumetric flow of butanol is larger compared to 4-compound mixture, which is the reason for higher pressure drop steady-state values.

Figure 5.4 shows zoomed response of pressure drop in reboiler to change of reboiler duty from 2 to 1.8. The pressure was measured for 2 hours to capture evolution of pressure after this change. It was assumed, that the three variables influence the overall pressure drop. These variables operate in different time regions. Vapor flow decreases immediately after lowering of the energy input, and the pressure drop decreases. Liquid flow decreases once the vapor flow is decreased, because the net amount of condensing vapor is lower. This phenomenon is slower, because the liquid load changes have to progress through the whole column. The slowest changes in pressure drop are caused by change of composition on column stages, as the temperature profile shifts with change of energy input.

First, fast drop of pressure difference immediately following the step in energy input is caused by lower vapor flow. The change of pressure drop has the biggest

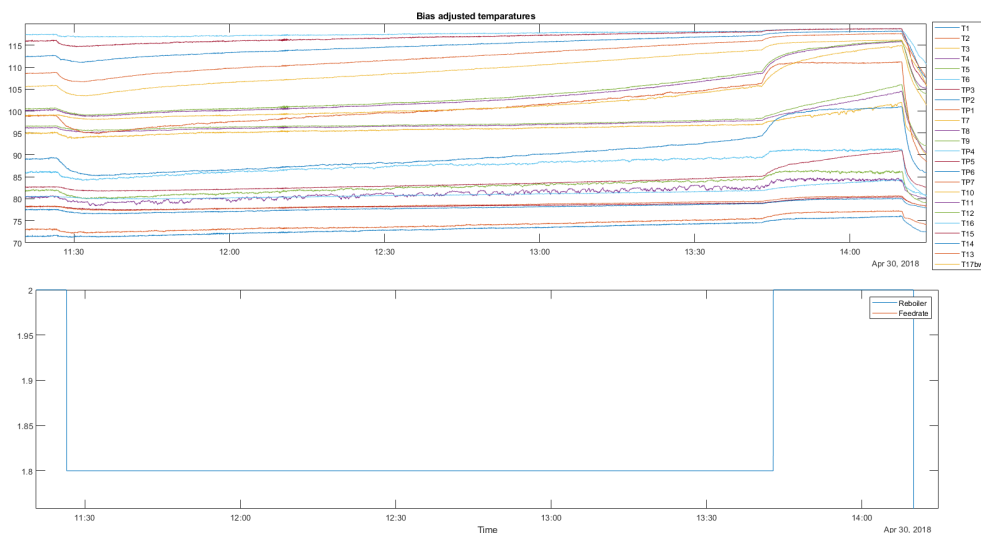


Figure 5.5: The temperature evolution, change in reboiler duty, 4-compound experiment, capturing evolution in time.

magnitude compare to other pressure evolution. This step is due to change of vapor flow. The slow increase from minimum to steady state value can be explained by combination of vapor and liquid flow; the change in vapor flow drop is fast, while the liquid load in the column is still height, the pressure drops to the minimal value, as the liquid flow is decreasing the vapor flow is slightly increased together with the pressure drop. The pressure drop is decreasing slightly during the remaining measurement time, this can be caused by the slow composition shift.

Correspondingly, temperature profile changes after introducing the change of reboiler duty. It is shown in figure 5.5. All temperature drops after step change from 2 to 1.8, the magnitude of this drop depends on position of the temperature measurement point. The bottom of the prefractionator is the most sensitive (TP6, TP7) with drop of 4-5°C, upper part shows weaker dependency, dropping to 0.9°C for TP1. The bottom of the column shows increasing trend in sensitivity, the temperature by reboiler T16 decreases for 0.5°C, while temperature measurement by the splitting of the column on prefractionator and main column (T17bw) drops about 2°C. The main column, and top of the column shows similar responses to induced change, the magnitude of this changes is ca 1°C for all measurements.

Experiment continues to observe slow changes at reboiler duty 1.8. Some of the temperatures are slowly increasing with time, the temperatures in bottom part of the column are getting closer to the temperature of reboiler. This increase is

observable for the bottom of the prefractionator and main column as well. The top of the column is heating up as well, but the slope is less steep.

This observation indicates the changes in composition profile. Some of the light products are escaping from the column, and heavier components (as butanol), are present in higher sections of the column. This would mean that less liquid is present in the column, and the amount of liquid in the reboiler is lower. This would explain the slow decrease of pressure drop during measurement. On the other hand, higher abundance of heavier components alongside the column would cause an increase of pressure drop, as the dependency of pressure drop on composition was presented by comparison of 4-compound and butanol experiments. Probably, the second effect is not that strong in comparison to the first one.

The step up in reboiler duty shows inverse dependencies to the first step described above, after this change the temperatures continue the slow increase due to composition change. Later, the reboiler duty is set to 0, and the cooling of the column starts.

The reasons for light components escaping are further discussed in Discussion.

### **Pressure Measurement by Feed, S1 and S2**

The measurement points located by feed entrance, side stream 1 and sidestream 2 are less advanced compare to reboiler measurement. The difference in liquid levels is deducted using millimeter paper and ruler. The measurement were not captured that often as well.

The change in pressure drop values of F, S1 and S2 measurements after reboiler duty step change are summarized in table. Both experiments, 4-compound and butanol are represented.

Pressure drop values for butanol experiment are higher in comparison to their 4-compound-experiment counterparts. The effect is most significant for high energy input. And similarly, the difference between S2 and F pressure drops is more visible for butanol experiments. For lower pressure, this difference is quite small.

The reboiler duty step change 2 to 1.8 for 4-compound experiments causes the total pressure drop decrease from 2 kPa to 1.1 kPa, the other pressures are similarly decreased to half of its value. The step back restores the values close to previous steady states, i.e. ca 1kPa for F and S2, and ca 0.8kPa for S1.

The butanol experiment shows reboiler duty step change from 2 to 1.8, and 1.8 to 1.6. In the first case, reboiler pressure drops from 2.4 to 1.3 kPa, while S1, S2 and F decreases accordingly. The pressure drops F, S1, and S2 at reboiler duty 1.6 are low and the values are difference between them is small.

Reboiler duty -	$\Delta p$ Reboiler [Pa]	$\Delta p$ F [Pa]	$\Delta p$ S1 [Pa]	$\Delta p$ S2 [Pa]
butanol experiments				
2	2.03	0.85	1.06	0.99
1.8	1.19	0.41	0.52	0.51
1.8	1.12	0.35	0.46	0.45
2	2.03	0.73	0.92	0.85
2	2.06	0.75	0.96	0.93
4-compound experiments				
2	2.4	0.85	1.06	0.99
1.8	1.3	0.43	0.58	0.51
1.8	1.3	0.43	0.58	0.451
1.6	0.6	0.09	0.14	0.18

Table 5.1: Pressure drop measurements for measurement points by reboiler, feed inlet (F), product side stream 1 (S1) and product side stream 2 (S2). Change of reboiler duty.

### 5.1.2 Change from Whole Column to Prefractionator and Main Column

The dependency of pressure drop in reboiler on position of vapor valves was measured. The vapor split valve at main column branch was closed completely, so the vapor flows through prefractionator only, and oppositely the vapor split valve at prefractionator column branch was closed to measure pressure for main column. Experiments were carried with pure butanol, and for two different energy inputs. The results are summarized in figure 5.6.

#### Whole Column to Prefractionator

The vapor split main valve was closed at two different reboiler duties. The blue curve shows pressure difference in reboiler after change of vapor flow from whole column in to prefractionator only at reboiler duty equal to 1.8, whereas the same change at reboiler duty 1.6 is shown in red color.

At higher energy input, the pressure increases from 1.2 kPa to 1,67 kPa, the pressure is getting close to new steady state in less than three minutes. For lower reboiler duty the change goes from 0.6 to 0.8 kPa.

It is observed, that the change in pressure is larger for higher energy input, this could be explained by nonlinear dependency of pressure on energy input. That agrees with other observations, where some changes in pressure had higher magnitude for larger energy input, whereas for low energy input, these changes were not

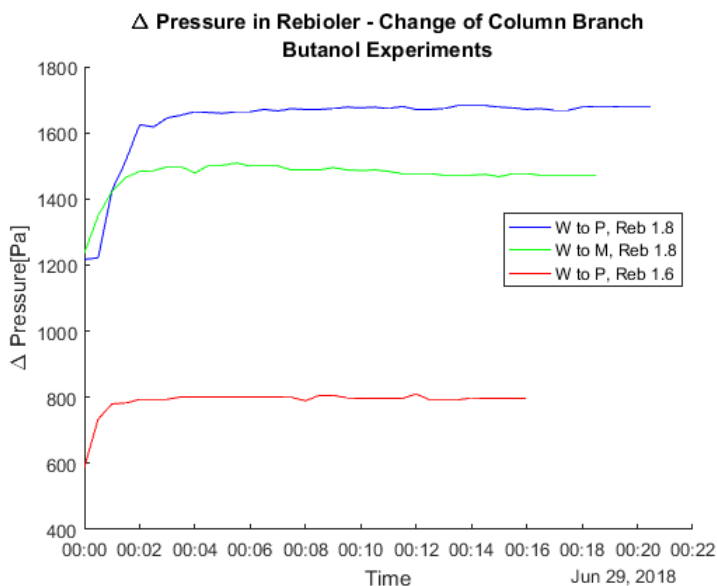


Figure 5.6: The pressure drop evolution, change in column branch: W – whole column, P- prefractionator, M-main column, reboiler duty at 1.8 and 1.6, butanol experiment.

observable.

### Whole Column to Main Column

The green curve shows the experiment, where vapor split prefractionator valve was closed at reboiler duty 1.8. The pressure drop in reboiler changes after the redirection of vapor flow from whole column to main column only. It causes following change of pressure change in reboiler; the pressure increases from 1.2 to 1.5 kPa reaching the new steady state in two minutes after initial step.

If the steady states pressure drops at prefractionator and main column are compared, the pressure drop in prefractionator is larger. It is due to different amount of packing in each of the branches. High of the packing in prefractionator, i.e. sections 1 and 2, is 2.7 m, whereas in main column, it is 2.1 m. The packing sections are smaller in main column, because there are internals installed for product side streams drain (liquid collectors, liquid split product valves), and these internals do not cause such a big vapor flow resistance as column packing.

The liquid split was at 0.5 during all experiments, so it should not interfere with results. The temperature profiles did not change much during the valve closing. The maximal temperature change were 0.2°C, the change is positive in the direction

of vapor flow, and negative in direction of its lacking.

It is ought to be noted, that due to conducting of other experiments, the opposite steps from branches to the whole column mode were not captured. These experiments, such as liquid split step changes, were usually stopped rather abruptly due to low level of butanol in reboiler, because some of it escaped through product streams during the experimental run. It is supposed that the steps, opening the respective vapor valves would have response opposite to what was observed during these experiments.

### **Pressure Measurement by Feed, S1 and S2**

The feed pressure drop measurement is situated in the middle part of prefractionator branch, while S1 is in upper third and S2 in bottom third of main column branch. This location is favorable for studies of pressure drop evolution after directing the vapor flow into one or the other branches.

Obtained results are summarized in table 5.2. Change of vapor flow from whole column to prefractionator causes decrease in S1 and S2, while pressure drop by feed increases for both tested reboiler duties.

The total pressure drop is increased as well, since the same vapor flow steams to more narrow passage in middle section. For 1.8 reboiler duty, the change in total pressure drop is 0.5 kPa, while increase by F measurement is 0.2 kPa. Feed measurement indicates part of the induced change, the pressure drop increase for upper prefractionator, section 1.

Step change from whole to main column at reboiler duty 1.8 causes total pressure increase by 0.25 kPa, the magnitude of S1 and S1 increase is 0.07, resp. 0.13 kPa whereas F drops from 0.49 to 0.4 kPa. This behavior agrees with assumptions.

The magnitude of changes is smaller for main column in comparison to prefractionator. This agrees with butanol experimental measurements, and proposed explanation about different packing heights.

### **5.1.3 Liquid Split**

The dependency of pressure drop on change of liquid split was studied.

#### **Total Pressure Drop**

The change of total pressure in reboiler due to liquid split change is described.

The pressure drop experiments for 4-compound mixture were carried, but no clear results were found. The responses varied incoherently for positive and negative

Reboiler duty	Branch	$\Delta p$ Reboiler [Pa]	$\Delta p$ F [Pa]	$\Delta p$ S1 [Pa]	$\Delta p$ S2 [Pa]
-	-				
1.8	W	1.18	0.29	0.44	0.46
1.8	P	1.67	0.25	0.34	0.464
1.6	W	0.59	0.09	0.14	0.18
1.6	P	0.80	0.04	0.07	0.25
1.8	W	1.22	0.30	0.47	0.49
1.8	M	1.47	0.37	0.59	0.40

Table 5.2: Pressure drop measurements for measurement points by reboiler, feed inlet (F), product side stream 1 (S1) and product side stream 2 (S2), change in column branch: W - whole column, P - prefractionator, M - main column, butanol experiment.

step changes. It is believed, that the reason lies in composition changes which effectively hides more subtle changes.

During butanol experiments, see figure 5.16, no direct effect of liquid split on total pressure drop was observed. The liquid split step changes for whole column, prefractionator and main column do not cause any measurable change. Pressure drop vary independently on induced steps.

All experiments were conducted at reboiler duty 1.8. The absolute values of pressure drop shows the already described effect of vapor direction into individual column branches. The curves for whole column experiments have different absolute values, this change in pressure drop during experimental day can be explained by decreasing of the amount of the liquid in reboiler.

### Pressure Measurement by Feed, S1 and S2

During pressure drop measurements for Feed, S1 and S2, no particular results were obtained. The results for 4-compound mixture are biased by composition shift. Butanol experiments do not show any results either, all pressure measurements follows the variation of total pressure drop, and these changes are not related to the liquid split changes.

#### 5.1.4 Heat-up

The pressure and temperature evolution during start up of the column was studied. The column is heated up at reboiler duty 2 with feed mixture inside the column. The heat-up experiment was conducted as a total reflux experiment where all the product streams were closed, and the feed was stopped.

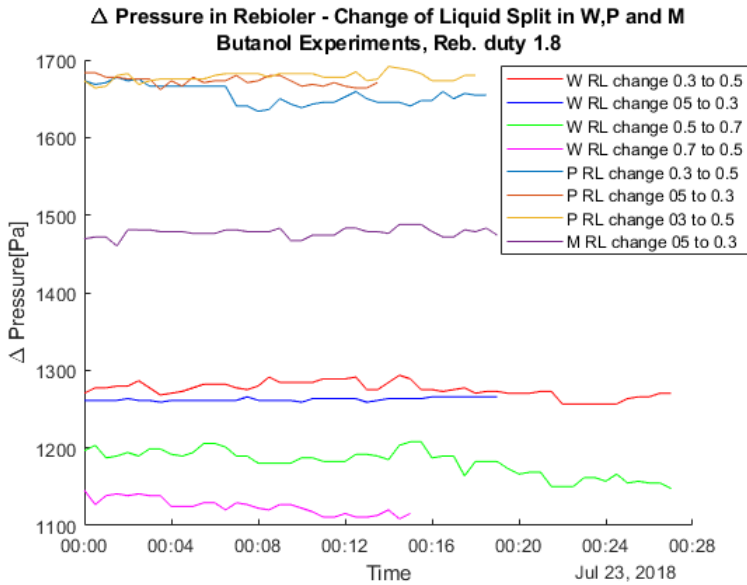


Figure 5.7: The pressure drop evolution, change in liquid split for whole column (W), prefractionator (P) and main column (M), butanol experiment.

## Temperature

The temperature increase and stabilization is captured in figure 5.8. The heating up of the column starts from energy source – the reboiler. The energy is used to heat up content in reboiler, about 8 liters of butanol with small amount of other alcohols from feed mixture. Once the temperature increases to about 100°C, most of the energy is used to vaporize liquid into vapor.

This vapor flows up and heats up sections above the reboiler, the vapor meets cold internals of the column, and condensates. Energy is used to heat up the column sections and internals. Its temperature increases up to the temperature of the vapor, the energy consumption depends on heat capacity of the internals and column walls. Once part of the column reach evaporation temperature, the vapor flow continue to the section above, and condensation occurs there on cold internals until the section is heated up.

Since the Kaibel column consist of two branches, the vapor has to split into prefractionator and main column. The vapor split ratio is naturally given by resistance of the packing and other internal parts, as well as by liquid split, or this ratio can be adjusted using vapor split valves.

From temperature measurements it is clear, that once the section is heated up,

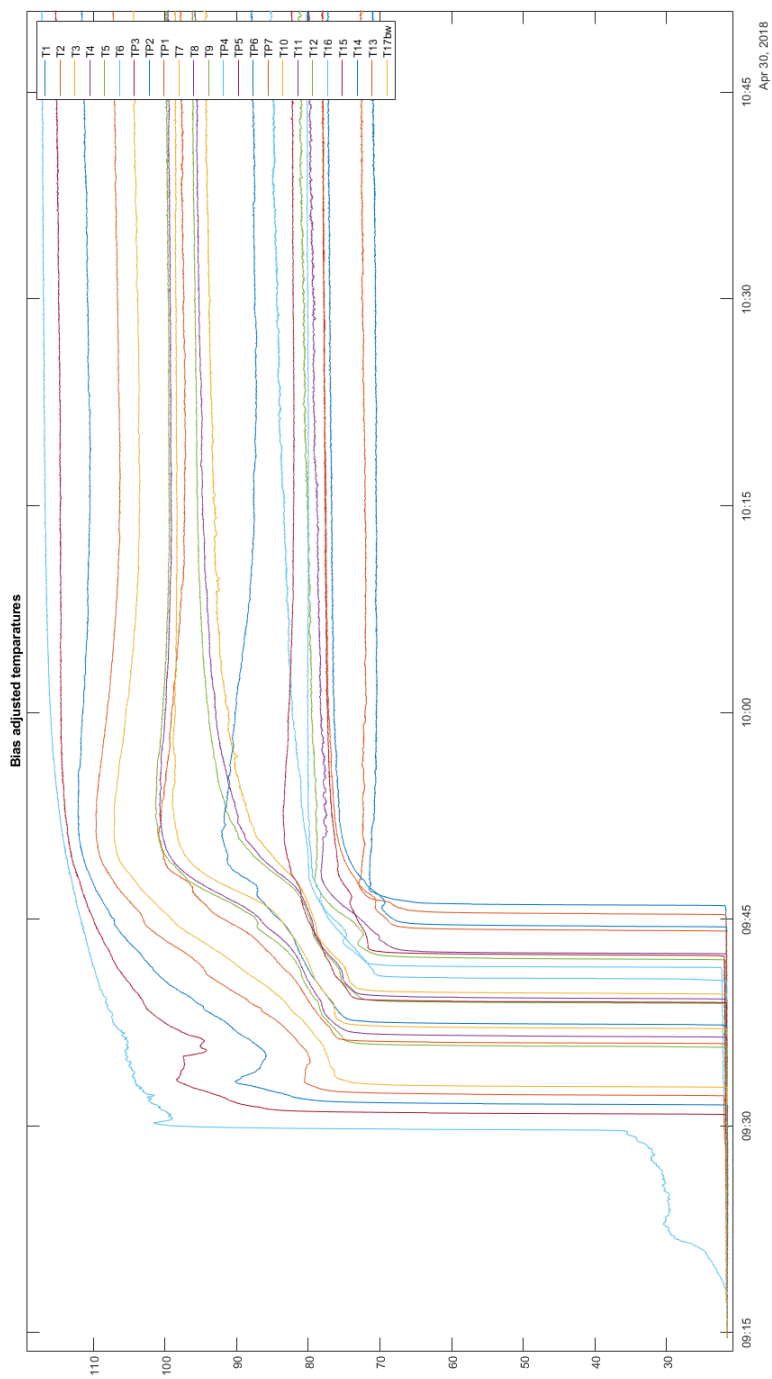


Figure 5.8: Heat-up of the column, and temperature stabilization during start up.

the temperature increase is fast as a step change, later this increase slows down, until the temperature settles on steady state. Once the top of the columns is heated up, the vapor enters total condenser, where it changes its state, and flows back into the column as a liquid. In figure 5.8, as T1 increases to stable point, most of the other temperature starts decreasing towards the steady state, or continues in increasing towards it.

The stabilization of the column into the steady temperature profile lasts ca one hour. It is clear from the figure, that the changes after initial fast increase for individual temperatures differ. This is due to diverse effects of vapor flow, and liquid flow in opposite direction. The change in liquid flow is induced by vapor flow, and naturally slower phenomena in general as liquid flows through the column.

## Pressure

Figure 5.9 shows pressure change in pressure drop.

The pressure increase started with the increase of T16 reboiler temperature. The increase slows down at 300 and 650 Pa, which agrees with the stop in increasing temperature in reboiler at about 30°C and 32°C. Then both, pressure and temperature start increasing again. Once T16 finishes the first jump, pressure is about 920 Pa, at the same time the T15 temperature starts increasing, followed by other temperatures. As the column is heated up, pressure drop increases, until the top is heated up (T1), and pressure drop stabilizes at maximum, 2.1 kPa.

Pressure drop is increasing with increasing of the height in the column, which vapor flow can reach before condensates.

## 5.2 Control Experiments

Different control structures for Kaibel distillation column were tested. Four to five feedback control loops regulates chosen temperatures alongside the column. The three loops are controlled using liquid split product valves D, S1 and S2. The fourth loop uses liquid split RL, or vapor split RV as manipulated variable. In 5-point temperature control, both vapor and liquid split in use.

### 5.2.1 Liquid Split Control

Closed loop experiments for 4-point temperature control were carried. TP5 temperature was used as a controlled temperature for liquid split control loop RL, the other three control loops use product valves D,S1,S2 as manipulating variables.

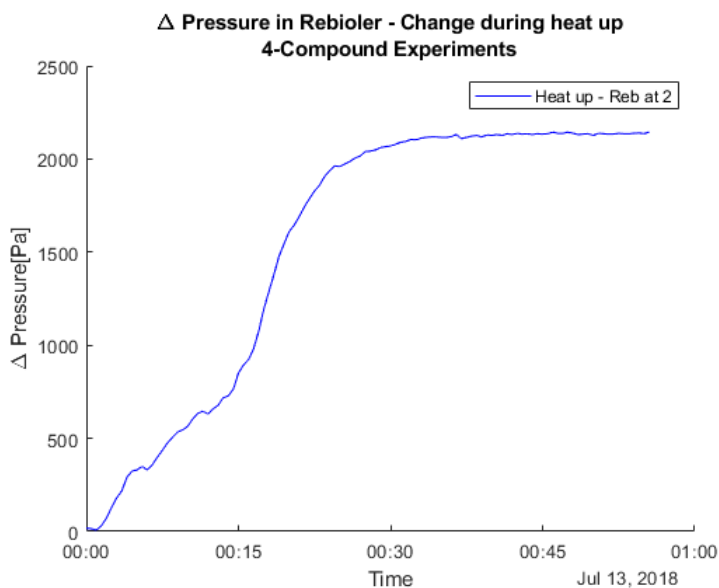


Figure 5.9: Heat-up of the column, pressure evolution during start up.

These experiments verify current controller settings, and serve as a comparison to other control structures. The response to setpoint changes of all controlled temperatures was measured together with rejection of disturbance of feed rate.

### Feed-rate Disturbance

The figure 5.10 shows disturbance of the feed rate of 20%. The feed rate was increased from 3 to 3.6 l/h at 9:38, and lowered back at 10:06.

In two minutes after the step change, the RL and S2 control loop are unable to keep the setpoint temperatures and start decreasing. Both controllers compensate for the disturbance, S2 temperature reaches desired setpoint in 10 minutes, while it takes more than 15 minutes for the RL. This is due to lower gain of RL controller. The magnitudes of the changes are 0.5 °C for both temperatures. Similar responses are seen for the step back.

The other control loops – D, S1 - seems unaffected, this is due to farther distance from the feed. Increase in feed rate causes higher load in the column. It is clear from the figure, that the S1 controlled temperature T7 is more noisy compare to the other temperatures, this is not due to difference of measuring device, but due to proximity of the top of the main column branch, where colder liquid meets warmer vapor, and temperature varies locally.

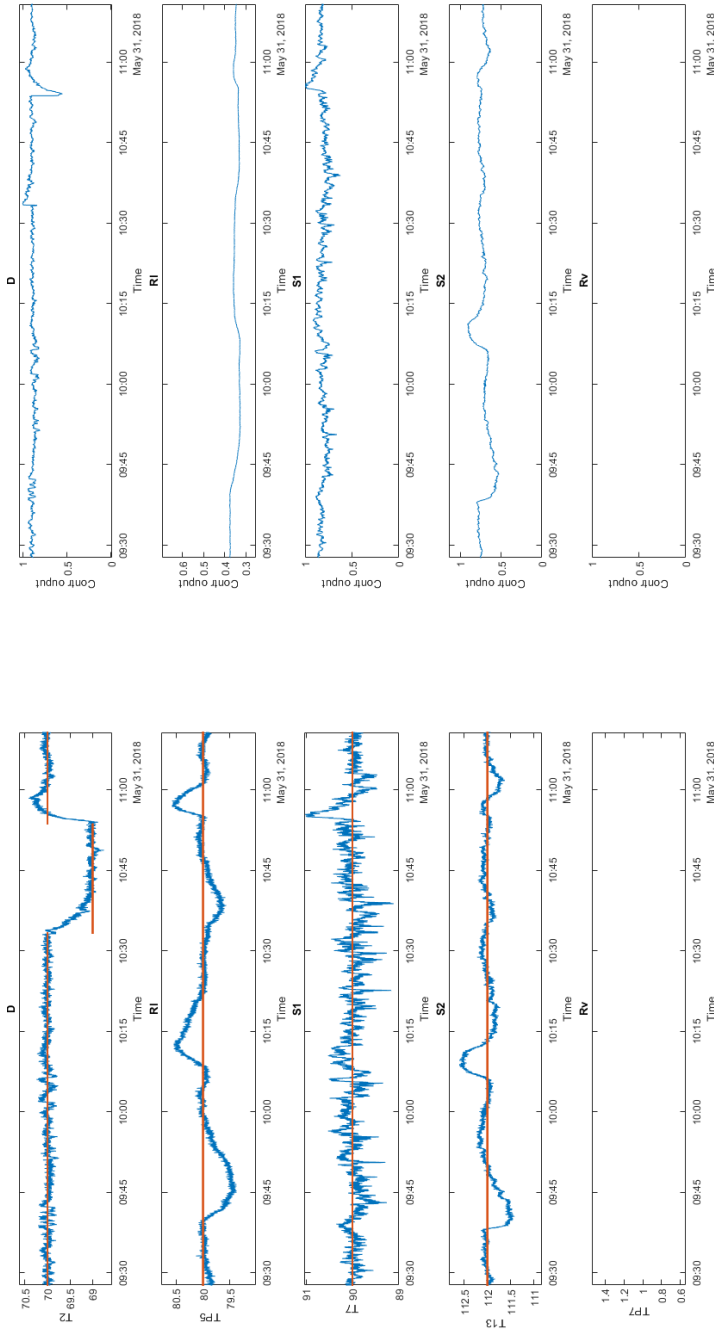


Figure 5.10: Closed loop experiments, 4-point temperature control liquid split, disturbance rejection: + 20 % feedrate at 9:38 and - 20% at 10:06, D setpoint change from 70°C to 69°C at 10:33 and back at 10:53.

The main disturbance is due to bigger load of colder feed entering the column. The feed temperature is around 40°C for temperature setpoint of feed heat element at 60°C. As the larger load is distributed through prefractionator, it affects RL temperature TP5 and continues down towards reboiler, where S2 temperature T13 is affected.

### **D Setpoint Change**

The same figure 5.10 shows the responses to change of setpoint in D temperature T2 from 70 to 69°C at 10:33 and 10:53 back. The D temperature reaches new setpoint in ca five minutes after initial change for both steps, for the step back the D temperature overshoots the setpoint. The effect on other loops follows.

RL temperature is driven away for ca five minutes, with magnitude of this changes less than 0.5°C in the same direction as D temperature changes. For S1 temperature, it is clear that some disturbance occurs the step down is not as visible in the noise, while step up shows increase in temperature for almost 1°C before it settles back in three minutes. The effect on S2 loop is rather small, following the same direction as RL with smaller magnitude, there is a small decrease in temperature after the second step, this can be explained by effect of other loops – RL, S1, which are settling.

The other loops are affected by the amount of liquid flowing from the top of the column, D manipulated variable.

The following figure 5.11 shows change in setpoints in variables RL, S1 and S2.

### **S1 Setpoint Change**

New temperature setpoint for S1, is reached almost immediately after the step at 8:54. The other temperatures are almost unaffected, smaller changes are visible for RL and S2 in the same direction, but this effect is so small, that it can be explained as well by variation due to change in composition.

### **S2 Setpoint Change**

The change in S2 temperature setpoint starts at 9:35, new setpoint is reached in ca 7 minutes. The response to step back is bit faster, setpoint is reached in 5 minutes without any overshoot. During the first step, the S2 manipulation variable saturates for initial response. These changes have no visible impact on the other control loops.

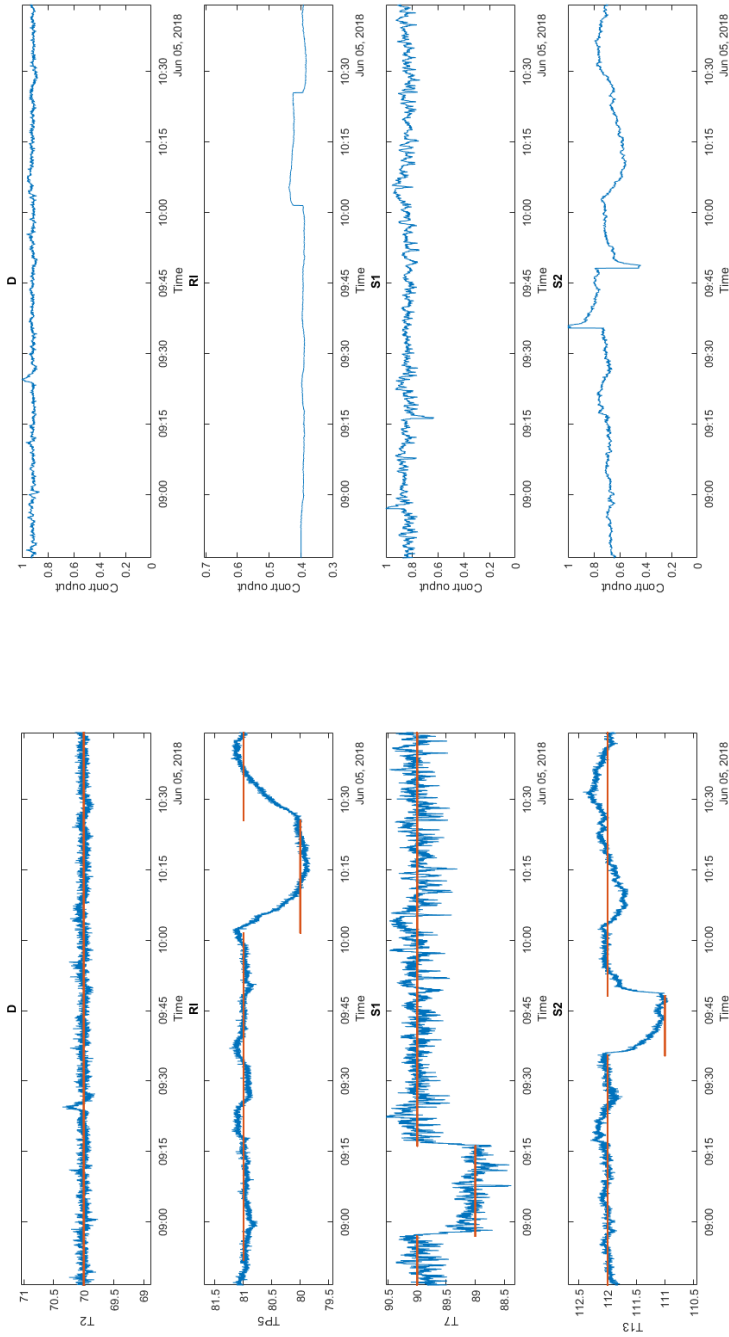


Figure 5.11: Closed loop experiments, 4-point temperature control liquid split, setpoint changes  $\pm 1^\circ\text{C}$ : S1 starts at 8:54, S2 starts at 9:35, RL starts at 10:01.

### RL Setpoint Change

At 10:01 the setpoint changes in RL were introduced. For step down, the new setpoint is reached after 10 min, for the step up the response is similar and it overshoots the setpoint first. This change has an effect on S2 controlled temperatures, while the other two are intact. The S2 temperature is disturbed in the same direction as the change of RL with the magnitude of  $0.3^{\circ}\text{C}$ .

To conclude, the manipulated variables are able to handle all of the introduced changes in reasonable time range. They operate in rather narrow range without getting saturated for most of the cases, which agrees with the sensitivity of controlled variables. The saturation in small scale occurs for S2 temperature change for initial response of the controller.

#### 5.2.2 Vapor Split Control

The usage of vapor split as a manipulated variable brings several challenges. As it was mentioned, two vapor split valves situated in prefractionator and main column enables the control of vapor split in whole range. The steps of valves are quite rough due to over-dimension of the equipment, and in several occasions, the slipping of the stepper motor, which moves the valves, was observed.

#### Open Loop

The open loop step response experiment was used to estimate the correct parameters for vapor split controller RV. The controlled temperature in RV loop is TP7 which is the most sensitive temperature, verified by experiments carried by Dwivedi (2013). The manipulated variable RV range from 0 to 1. This value is translated into position of the valves as explained in Experimental Setup.

The steps were conducted in whole range of RV, the response of TP7 is captured in figure 5.12. It can be seen that the magnitude of the responses are dependent on the position of the initial and final value of manipulated variable, i.e. the temperature change is nonlinear to the change of RV.

First, set changes were conducted close to the middle value of 0.5, which agrees with position where both valves are open. It can be observed, that the temperature responses are of small magnitude. The first high peak at  $115^{\circ}\text{C}$  was caused by lack of feed entering the column, and hides the response to the step change from 0.3 to 0.7. Later, the step changes were conducted closer to the edges of the RV range. The temperature responses has larger magnitude compare to previous step responses. The actual steps and temperature responses are summarized in a table 5.3.

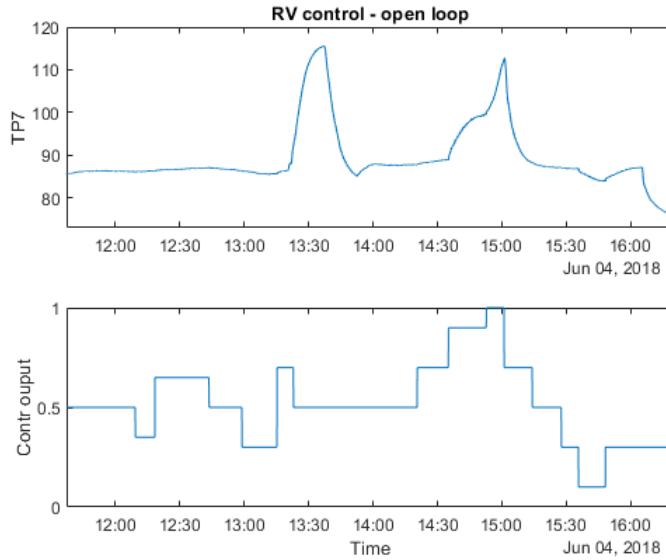


Figure 5.12: Open loop experiments, 4-point temperature control vapor split, RV step changes.

RV start - final	$\Delta TP7$ [°C]
0.5 – 0.35	no visible change
0.35 – 0.65	0.37
0.65 – 0.5	0.26
0.5 – 0.3	0.5
0.3 – 0.7	disturbance
0.5 – 0.7	0.5
0.7 – 0.9	6.3
0.9 – 0.1	unstable
0.5 – 0.3	0.3
0.3 – 0.1	2.9

Table 5.3: RV Open loop step changes,  $\Delta TP7$  response after 5 minutes from the initial change.

### Controller Tuning

It is clear, that the magnitude of TP7 temperature responses towards RV varies along the range of manipulated variable. This change of sensitivity, can be also concluded from active vapor split experiments presented by Dwivedi (2013). Their controller tends to keep the RV at positions close to the boundaries on both sides, where the temperature is more responsive, while the middle range is almost unused.

This causes difficulties to find correct parameters of the controller. The controller gain  $K_P$  is dependent on the step position, therefore the computed values varies from 0.09 for the edges to 10 for the middle range.

Different controller settings and boundaries of manipulated variable were tried. To summarize the observations:

- For large gain the temperature responded for changes close to middle range, but was unstable for changes close to the edges.
- For smaller gain, the responses at the middle range are not observable, and the controller tends to saturate in one of the extremes, and doesn't reach the desired steady state.
- RV boundaries 0.1 – 0.9 were used in most of the experiments to avoid complete closing of vapor flow through one of the branches. Experiment with lowering of the boundaries to 0.3 – 0.7, and thus usage of middle range only, in combination with large controller gain did not bring desired effect.

It was conceded, that the main problem lies in the uncertainty of the responses in the middle range, where the switch between vapor split valves occurs. It was assumed, that some nonlinearity could be removed by using one valve only for control of the vapor split, and lower the RV range to one half.

From open loop experiments, it is concluded that the controlled temperature TP7 is more sensitive towards the changes of RV in its upper range. Note, that observation of the last open loop steps 0.5 - 0.3 and 0.3 - 0.1 could have been biased due to big disturbance caused by previous step 0.9 - 1. Even if the sensitivity is the same for both valves, the possibility of measurement bias justify the choice.

Therefore, the boundaries of manipulated variable RV were set  $<0.5, 0.9>$ , which means regulation of the vapor slit by split valve in the main column only.

The controller parameters were computed from the step change 0.7 to 0.9. The SIMC rules for integrating processes (Skogestad (2003)) were used. The parameter estimation for  $\tau_{au_c} = 2min$ , results in  $K_P = 0.09$ ,  $\tau_I = 8$ . This controller would be able to cover the changes close to upper boundary, due to small gain, but would not be that responsive at lower part of the range.

The setpoint temperature for controller was found by setting RV to manual control at value 0.7. To avoid temperature drift and maintain control of the prefractionator, the RL control of TP5 was turned on. Once, the steady state was reached, the RL control loop was turned to manual, and RV control loop was turned to on.

### **RV Setpoint Change**

From figure 5.13, it can be seen that RV controller is able to keep steady state. The step change of RV controlled temperature TP7 was introduced. The response to step up is rather slow, controller steps from 0.7 to 0.8 almost immediately, but it takes more than 15 minutes to reach new setpoint. There is visible pause, where temperature stops increasing, this can be due to delay in between proportional and integrating action of the controller, or due to some disturbance in feed composition. The other control loops are unaffected by this change.

The TP5 temperature increases as the temperature in whole prefractionator arise with larger vapor flow. The temperature responses for change of vapor flow were captured, and are presented in Appendix B. To conclude, the temperature in prefractionator increases with step up, and decreases with step down, the effect is largest at the bottom of the branch, whereas at the top of it the change is hardly observable. The main column seems unaffected by this changes, temperatures in the bottom of the main column varies, but no visible trend is observable.

The step down in setpoint is faster compare to step up, in 10 minutes temperature is close to new steady state. However, the temperature stays ca 0.3°C higher than the steady state, the controller is unable to reach it in observed time range. During the step down, RV manipulated variable reach values around 0.6, where the temperature sensitivity to RV change is weak.

### **RL Disturbacne**

The controller settings were tested for capability of disturbance rejection. The step change of liquid split RL was introduced into the system, see figure 5.14. The step from 0.4 to 0.45, increased the liquid load into the prefractionator. TP7 controlled temperature decreases from steady state for five minutes, with the lowest value differing from setpoint about 1.5°C, before it starts increasing and reach setpoint in ca 10 minutes. The S2 controlled temperature T13 follows the same trend with lower magnitude.

The manipulated variable increases before it almost saturates, and stays at 0.88. After the disturbance is introduced, the oscillations of the controlled temperature

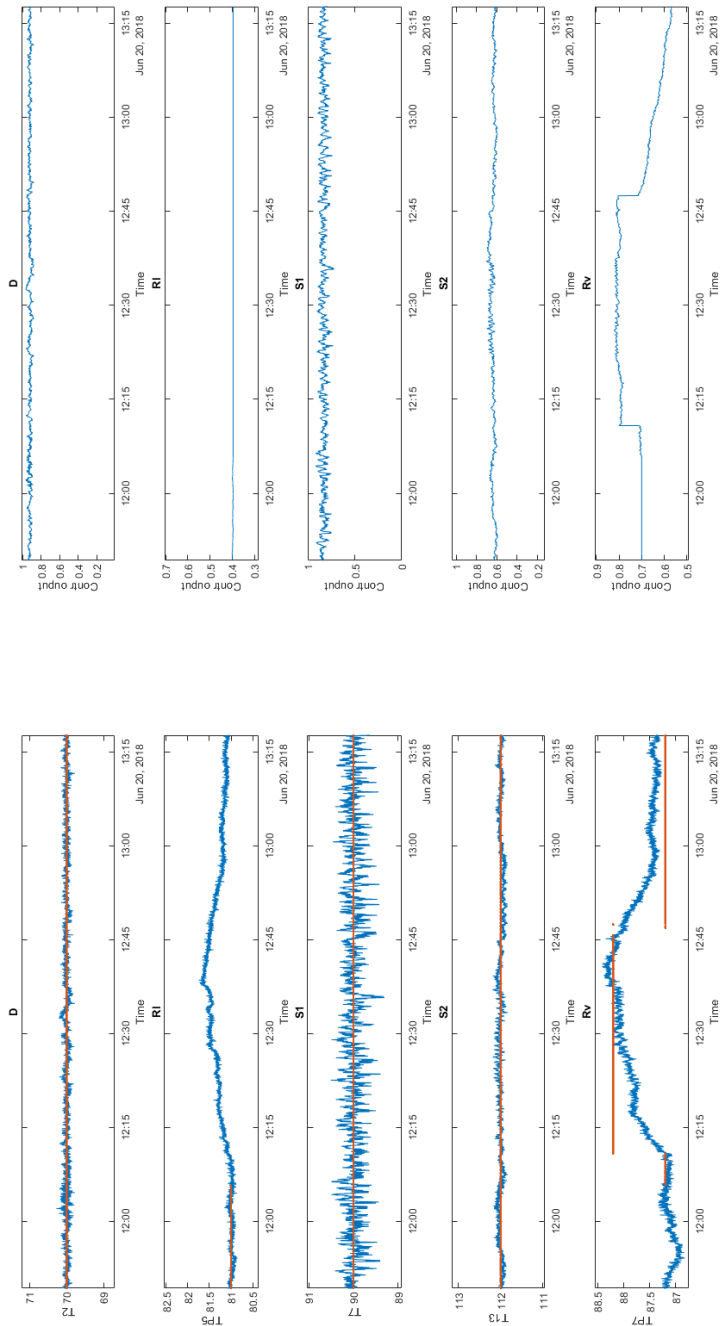


Figure 5.13: Closed loop experiments, 4-point temperature control vapor split, TP7 step change.

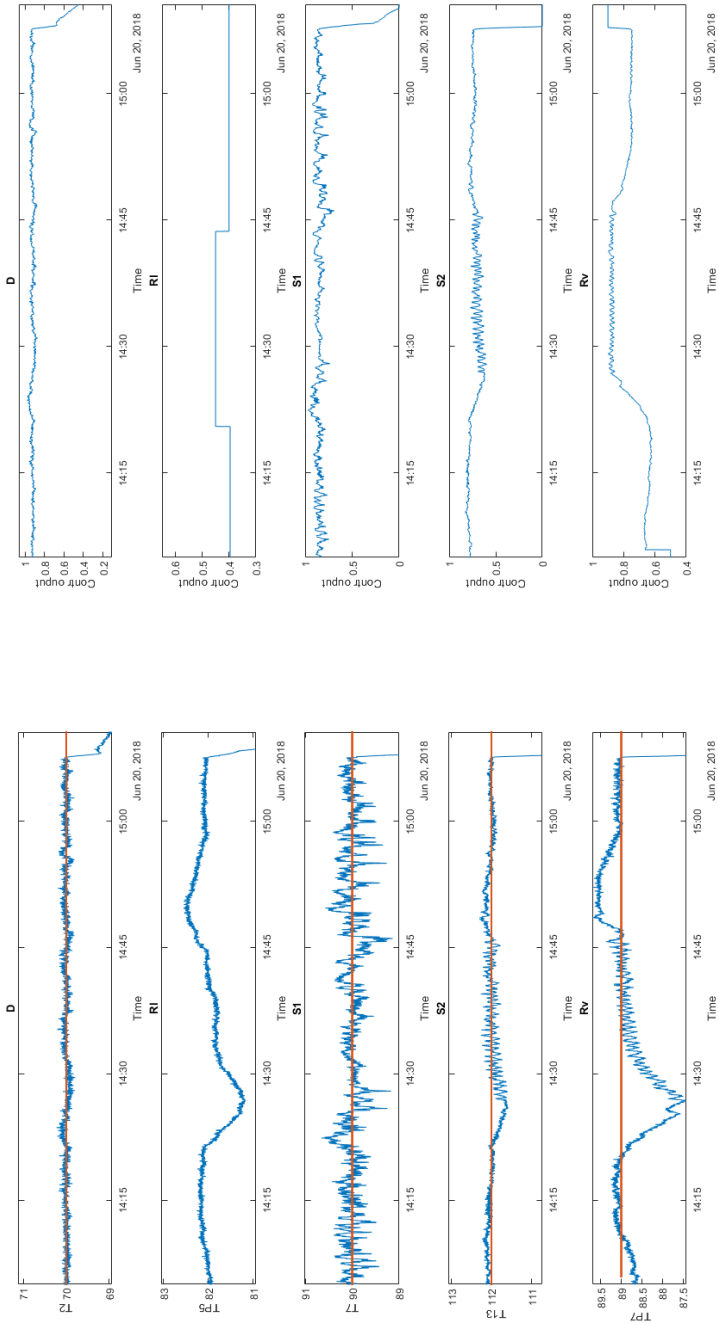


Figure 5.14: Closed loop experiments, 4-point temperature control vapor split, RL disturbance.

occur. The oscillations are locally distributed in the system, which is visible from oscillations of the S2 controlled temperature, but not from the others.

RV at 0.9 means that most of the vapor flows into prefractionator, as vapor split valve in main column is almost closed.

The RL step from 0.45 to 0.4, decreases the liquid load, and TP7 increases about  $0.5^{\circ}\text{C}$  before it settles back in ca 10 minutes. The oscillations disappear, as RV controller decreases from saturation. This trend can be seen for S2 temperature as well.

From the system reaction to RL at 0.45, stabilization of RV close to its limit can be concluded that for given settings the system is on the edge of stable operation. Settings includes feed rate, energy input, controller settings, boundaries of manipulated variables, and setpoint temperatures.

In this case, the newly introduced were RV controller settings and boundaries, and RV temperature setpoint. The setpoint temperature was set the same way as for RL controlled temperature; after start up, manipulated variable was kept at desired steady state value manually, until the temperature settles, and then the control loop was introduced. The temperature profile of prefractionator is strongly dependent on feed composition, which slightly vary from batch to batch. For these experiments, batch is formed by recycling products from product tanks and by removing part of the butanol which accumulates in reboiler during operation.

The lowering of setpoint temperature would allow to move from the saturation and avoid oscillations.

### **S2 Setpoint Change**

The setpoint change for S2 controlled temperature T13 was introduced into the system, see figure 5.15 The new steady state was reached after five minutes from the initial step change at 9:58. The RV controlled temperature TP7 lowered below setpoint, but not immediately after the step change, thus there could be other reasons for this behavior. During this step, some small oscillations of RV, D and S1 controlled temperatures occurs. This oscillations stays after the step change in S2 setpoint back to initial value. It takes 15 minutes for S2 temperature to reach the desired value after step back, the TP7 is increased temporarily to  $90^{\circ}\text{C}$  after the new steady state of S2 is reached.

It can be concluded that, while the controller settings are not ideal, it is possible to reject setpoint changes and disturbances in reasonable time. The controller's optimal value lays in good operating range, and avoids saturation, and complete closing of the vapor valves.

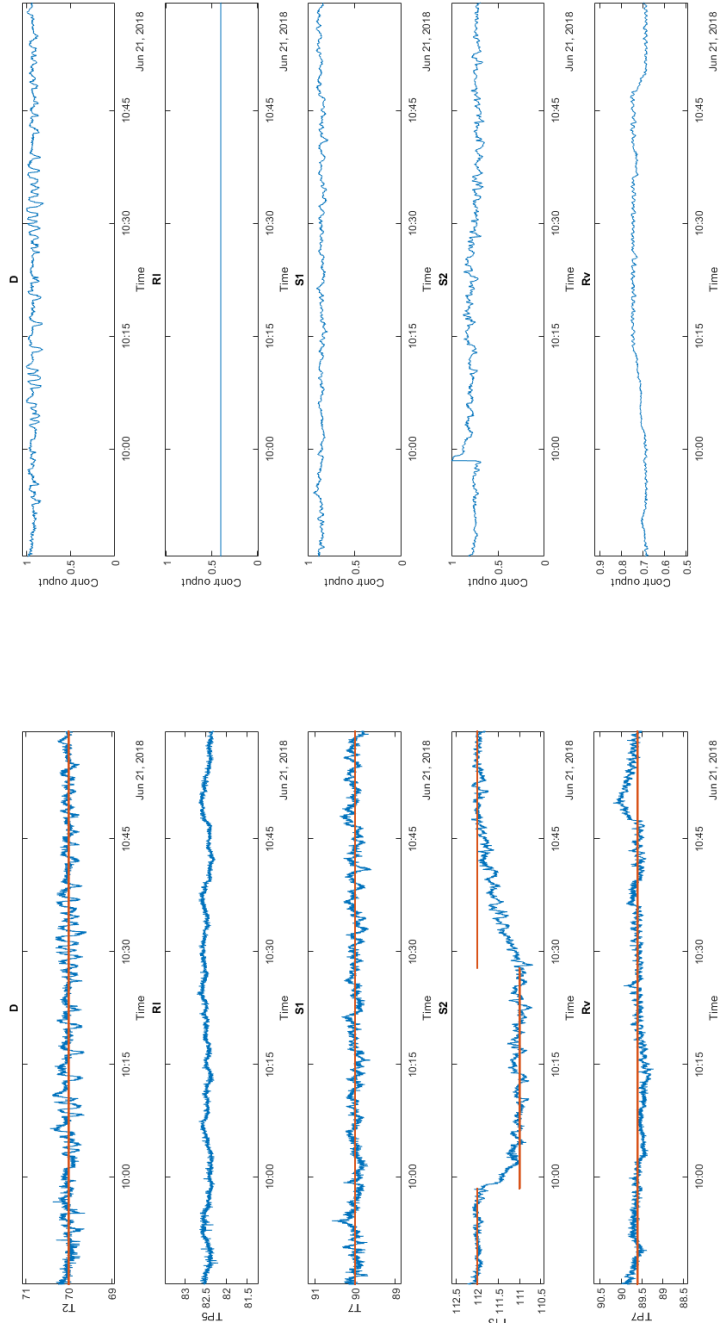


Figure 5.15: Closed loop experiments, 4-point temperature control vapor split, S2 step change.

Oscillations were observed close to the upper boundary for RV. This can differ for various setpoints for TP7. The other reason could be rather narrow boundaries for liquid split RL (and chosen steady state). This idea is covered in Discussion.

### 5.2.3 5-point Temperature Control

Experiments were carried to verify new control structure, which was introduced to improve the control of the column. The goal was to use two different temperatures in prefractionator as controlled variables for two separate control loops to improve the speed of stabilization of the prefractionator temperatures. The manipulated variables available to use are liquid split RL and vapor split RV. The vapor split control temperature is the same as in previous experiments, TP7 on the bottom of the column is the most sensitive temperature for vapor split. The same controller settings were used as in previous case. The possible temperatures for liquid split control were TP1 to TP6. Temperature TP5, the most sensitive one towards the RL, was declined due to high sensitivity towards the change of vapor split, and the same reasoning applies to TP6. The two control loops would contradict each other. TP4 is temperature measurement by feed entrance, therefore the temperature variations are rather large and the temperature is most sensitive to disturbances in feed rate, its temperature and composition, which summarize the reasoning against using this temperature. TP3 measurement sensor is strongly biased, unavailable for control purposes. The remaining temperatures TP1 and TP2 have similar sensitivity towards RL variations, and the influence by vapor split variation is smaller compare to TP5. Both temperatures seems as acceptable choices for control variables.

#### Open Loop Experiments

As the first open loop experiments, figures 5.16 and 5.17 showed varying result, more experiments were conducted to uncover the behavior. For experiments on figures 5.16 and 5.17, S1 and S2 control loops were turned on.

Figure 5.16 shows temperature responses of TP1, TP2 and TP5 to step in RL. After the first step change, RL from 0.5 to 0.3., the TP5 temperature starts increasing; both TP1 and TP2 show small inverse response before start increasing. A smaller RL step in opposite direction induces decreasing of all studied temperatures.

In figure 5.17 is shown rest of the results from the same laboratory run. The RL step change from 0.5 to 0.4 and back is introduced to the system. TP5 increases and decreases accordingly. The response from TP1, and TP2 is weak, again the

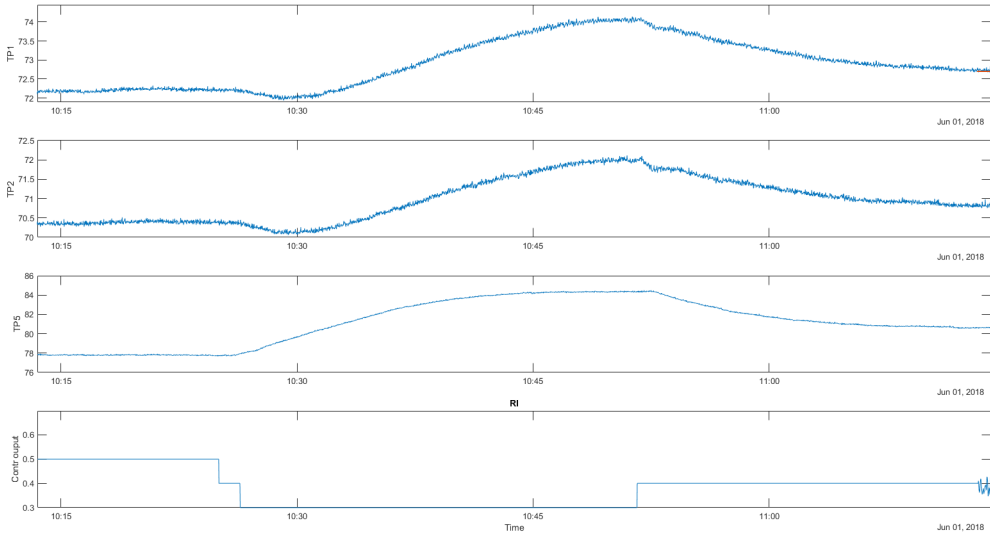


Figure 5.16: Open loop experiment, 5-point temperature control, RL step change, TP1, TP2 and TP5 responses, closed loops D, S1, S2, open loop RV.

inverse response is observed. In this case, this inverse response last longer compare to previous figure, and its magnitude is almost larger than the rest of the step.

The other set of experiments were carried to uncover the changes. The control loops S1 and S2 were set to manual at steady state values to eliminate the influence of respective control loops. RL was changed from 0.4 to 0.6 and back, see figure 5.18. The TP1 and TP2 temperatures show yet another not predicted behavior. As the RL is increasing, the temperatures start responding in “correct” direction (the same as TP5), but then starts increasing until reach peak and lowers bit again, where it settles. After RL step from 0.6 to 0.4 is introduced, TP1 and TP2 starts decreasing, the minimal values are reached and then increase towards steady state.

In comparison to other controlled temperature, the TP1 and TP2 copies the response of S1 controlled temperature T7, and consequently D controlled temperature T2. Since the S1 loop was on manual, the liquid split change influenced T7 and caused variations, which were distributed to prefractionator.

The last open loop experiment was conducted with all control loops closed, namely D, S1 S2 and RV. Results are presented in figure ZZ. TP1 and TP2 shows similar behavior as TP5 with smaller magnitude. After five minutes from original change, the open loop responses are reversed by RV control, which tries to remove the liquid split disturbance. The controller settings were calculated from initial

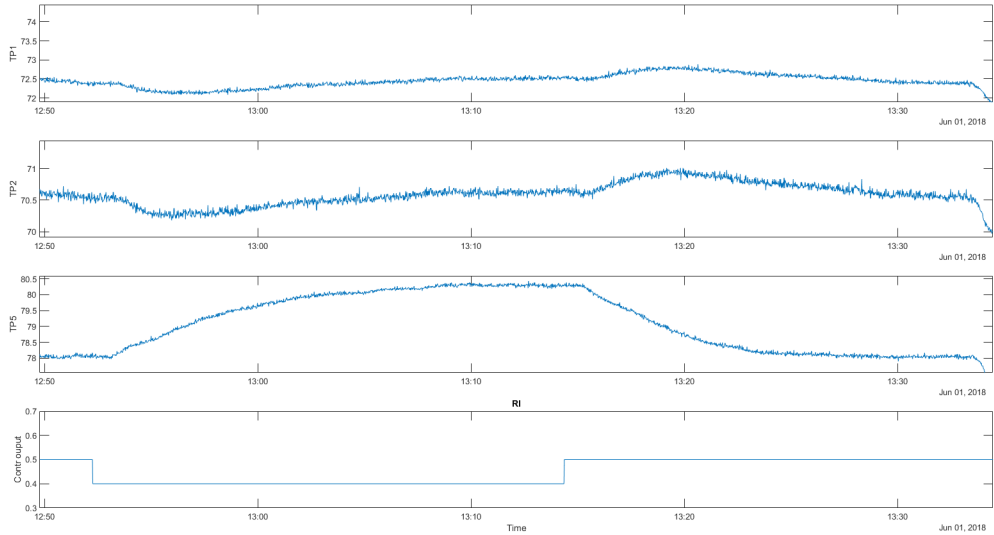


Figure 5.17: Open loop experiment, 5-point temperature control, RL step change, TP1, TP2 and TP5 responses, closed loops D, S1, S2, open loop RV.

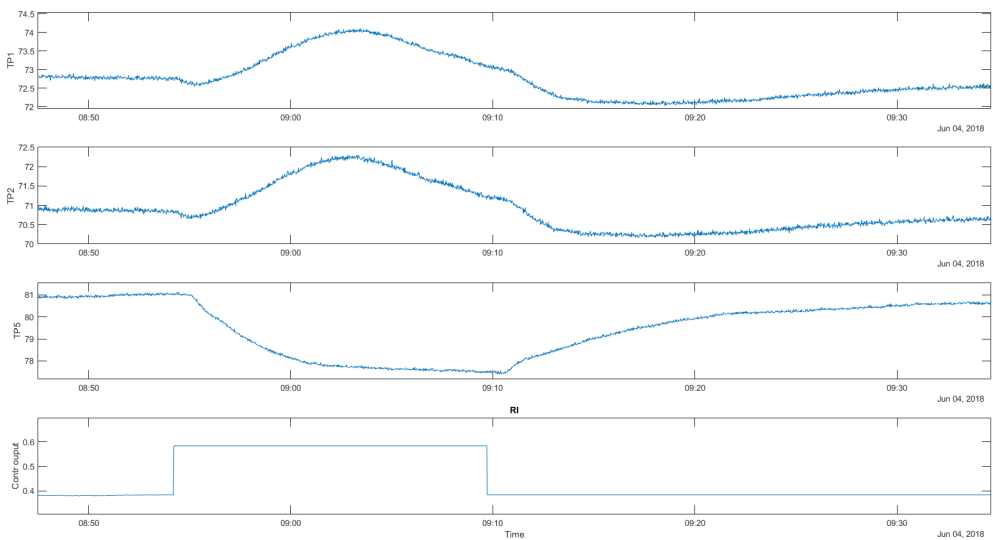


Figure 5.18: Open loop experiment, 5-point temperature control, RL step change, TP1, TP2 and TP5 responses, closed loop D, open loops S1, S2, RV.

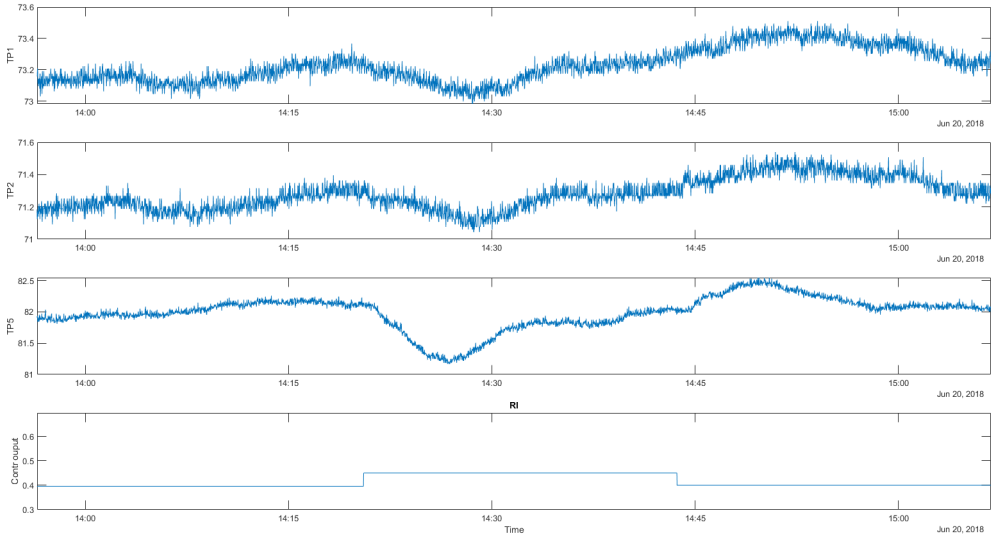


Figure 5.19: Open loop experiment, 5-point temperature control, RL step change, TP1, TP2 and TP5 responses, closed loops D, S1, S2, RV.

responses.

### Controller Tuning

The SIMC rules, by [Skogestad \(2003\)](#), were used to find the controller parameters.

Two different values of  $\tau_c$  parameter were tried. Controllers with  $\tau_c = 1min$ , were too fast, and the liquid split variations were too big – changing from 0.3 to 0.6 every couple of minutes. This would cause big variations inside the column, and even instability.

For  $\tau_c = 2min$ , the parameter the RL variations are lower. The controller with parameters  $K_P = -1$ , and  $\tau_I = 8$  is shown in figure 5.20. TP1 controlled temperature is increasing, but the increase of manipulated variable RL seems to only worsen it. Then, RL is set to manual. It seems that for bigger variations of liquid split RL, the “inverse” response prevail, and temperature TP1 shifts in the direction of T7 change.

### 5.2.4 Pressure Drop Modeling

Simulation results are summarized in table 5.4. The pressure values are smaller compare to experimental results. This can be due to the used equation, which was derived for columns with larger diameter. From experimental studies on random

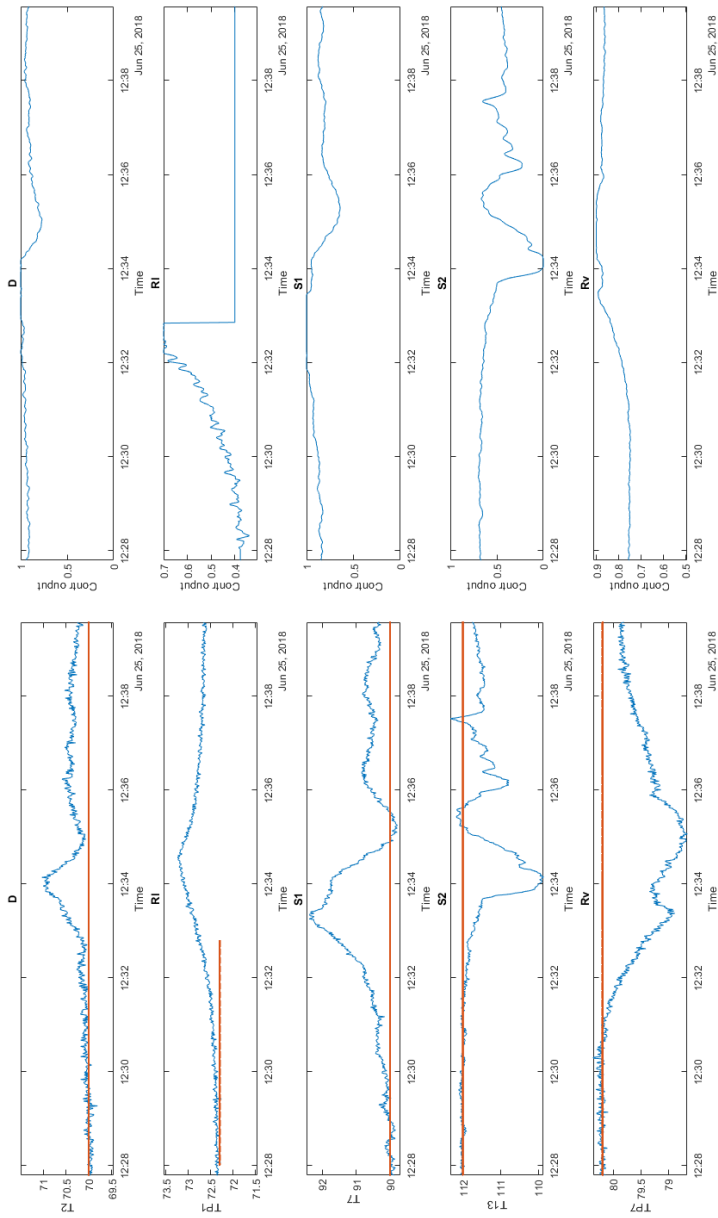


Figure 5.20: Controller Tuning, 5-point temperature control, controlled temperatures and controller outputs vs. time

Table 5.4: Results for pressure drop modeling

Reb. duty	RV	total pressure	pressure P	pressure M	molar flow P	molar flow M
-	-	[Pa]	[Pa]	[Pa]	[mol/s]	[mol/s]
2	0.5	455	98.15	98.15	0.0225	0.0266
2	0.3	456.3	98.89	98.89	0.0224	0.0267
2	0.1	457.67	99.6	99.6	0.0223	0.0268
2	0.7	457.63	99.37	99.37	0.0226	0.0264
2	0.9	460.17	100.56	100.56	0.0227	0.0263
1.8	0.5	265.7	57.31	57.31	0.0172	0.0203

packing, it is known that the dry pressure drop is smaller for smaller column diameters. Parameter can be introduced into the pressure resistance equation for fitting of the model to experimental results. The model shows expected results for change of reboiler duty, and the vapor split change.

## Chapter 6

# Conclusions, Discussion, and Recommendations for Further Work

### 6.1 Discussion

The discussion chapter focus on description of peculiar behaviors, the most relevant discussion is in Result section.

#### **Pressure Measurement by Vapor Split Valves**

The valves are equipped with two horizontal tubes with ca 5mm in diameter. Pressure measurements were realized using silicone hoses molded in U-shape with one end connected to the horizontal tube emerging from the vapor valve, and with the other end open to the atmosphere.

It was observed, that some liquid was accumulated in these tubes, and also partially in hoses. The main reason for it is seen in condensation of vapors in narrow passage, where it stays and eventually forms liquid plug, which biases the measurement. Capillary forces can be other reason for liquid accumulation, probably these forces enhances the first effect.

There were several signs, that measured values were incorrect. The two measurement points, PB and MB, which denotes the pressure bellow respective vapor valves, sometimes differ, even-though the measured pressure should be equal, since there is no packing or other internals between these two points. Also, as the lab-

oratory run progressed in time, the measured values were getting lower, and some even got into negative, which would indicate pressure in the column lower than in atmosphere.

### **Pressure Buildup by Side Stream 2**

Different approaches were introduced to en light the phenomena of pressure build up and pulsating. The pressure build up was observable on liquid seal by side stream 2 (S2), which is also used as pressure measurement. The pressure increases, sometimes in form of pulses. Once the liquid seal is overcome, the vapor is leaking from the column through S2. The pressure increase is distributed inside the column, the vapor leakage stops the vapor flow into the upper part of prefractionator.

The larger liquid seals to were equipped to the column for S1, and S2. The effective height of these U tubes is ca 35cm. During experimental run, even these new liquid seal was overcome. This observation denotes pressure equal to more than 35cm of height of liquid column. In comparison, the normal liquid column height for total pressure drop in reboiler for this operation is ca 25-30 cm. Since the pressure was larger, than total pressure drop in whole column, the source of pressure build up has to be external.

Finally, the pressure phenomena was explained. The S2 product tube is quite narrow, and on its way to product tank has to do two 90° turns, and leads almost horizontally. The tube was replaced by wider silicone hose, and it was observed that the liquid is accumulated above the entrance to the tank. The problem lies in small throughput of the tank. When the liquid plug is formed and the pressure by S2 is increasing.

### **Experiment – Model Mismatch**

The simulation results show that model describes the phenomena rather well, but the magnitude of these changes is low. In [Maćkowiak and Maćkowiak \(2014\)](#) is written that - for random packing - the dry pressure drop depends on the diameter of the column. This could explain the experiment-model mismatch. Parameter can be introduced for better fit.

The other option could be that the chosen approach for estimation of pressure restrictions is unsuitable for given experimental column. The empirical equation is denoted for columns with considerably larger diameters.

## 6.2 Conclusions

The theoretical part provides introduction to problematic of Kaibel column, dividing wall columns, and other thermally coupled arrangements with focus on control approaches. The practical implementations of vapor split control were shown. The other part focus on pressure drop, and different approaches of pressure drop estimation and modeling.

The pressure drop evolution in Kaibel column was studied experimentally. The pressure drop is strongly dependent on energy input. The total pressure drop increases, if one of the branches is closed, and the magnitude depends on amount of packing in given section. The composition is also important factor for pressure drop, the feed with higher molecular weight, the pressure drop is higher. The change of liquid split does not have particular influence on pressure drop.

The model for pressure drop in Kaibel column was created. The model is able to compute steady state values for total pressure drop, pressure drop in prefractionator, and main column, and vapor flows into respective branches. The input variables are reboiler duty, vapor split and temperature and composition in reboiler. The simulations show expected dependency on reboiler duty and vapor split. The model was not fitted to experimental data.

The four-point temperature control of Kaibel column was studied. Control structure with liquid split control can reject feed disturbances, and setpoint changes of all variables.

The control structure with vapor split was introduced, and the open loop responses were studied. The sensitivity of controlled temperature is strongly dependent on the position of the step change in manipulated variable. The controller was tuned using only one of the valves to avoid non-linearity in responses, and avoid saturation at boundaries. Even for this one-valve-control, the system was able to reject setpoint change, liquid split disturbance and setpoint change of side stream 2 control loop temperature.

The five-point temperature control of Kaibel column was studied. The addition of second control loop to the prefractionator enables both liquid and vapor split control. The open loop responses for preferred controlled temperatures in prefractionator were conducted. The temperatures on top of the prefractionator show incoherent responses, and the strong dependency on control loop S1 was found. The sensitivity towards the liquid split is rather low. The steady operation closed loop operation for 5-point control was not reached.

### 6.3 Recommendations for Further Work

- Re-tune vapor split controller for wider rejection
- Try other controlled temperatures for five point control
- Fit the pressure model to experimental data

# Appendix A

## Acronyms and Abbreviations

**DWC(s)** Dividing wall column(s)

**GDPR** Generalized pressure drop correlation

**B** Bottom product

**D** Distillate, top product

**RL** Liquid split

**RV** Vapor split

**S1** Upper side stream product

**S2** Bottom sidestream product



# Bibliography

- Billet, R. (1995). *Packed towers in processing and environmental technology*. VCH.
- Billet, R. and Schultes, M. (1991). Modelling of pressure drop in packed columns. *Chemical Engineering & Technology*, 14(2):89–95.
- Duss, M. (2013). Packing pressure drop prediction at low operating pressure - is there anything new?
- Dwivedi, D. (2013). *Control and operation of dividing-wall columns with vapor split manipulation*, Ph.D. thesis. PhD thesis, Norwegian University of Science and Technology, Department of Chemical Engineering, Trondheim, Norway.
- Dwivedi, D., Halvorsen, I. J., and Skogestad, S. (2012). Active vapor split adjustment for energy optimal control of dividing wall distillation columns: Experimental studies. In *Trondheim Gas Technology Conference*.
- E. Brunazzin, A. P. (1997). Mechanistic pressure drop model for columns containing structured packings. *AIChE Journal*, 43(2):317–327.
- Eckert, J. S. (1975). How tower packings behave. 82:70–76.
- F. B. Petlyuk, V. M. Platonov, D. M. S. (1965). Thermodynamically optimal method for separating multicomponent mixtures. *International Chemical Engineering*, 5((3)):555–561.
- Ge, H., Chen, X., Chen, N., and Chen, W. (2014). Experimental study on vapour splitter in packed divided wall column. *Journal of Chemical Technology & Biotechnology*, 91(2):449–455.
- Giroux, V. A. (1980). Fractionation method and apparatus.
- Halvorsen, I. and Skogestad, S. (2006). Minimum energy for the four-product kaibelcolumn. *AIChE Annual meeting*.

- Halvorsen, I. J. and Skogestad, S. (1999). Optimal operation of petlyuk distillation: steady-state behavior. *Journal of Process Control*, 9(5):407 – 424.
- Joon Kang, K., Harvianto, G., and Lee, M. (2017). Hydraulic driven active vapor distributor for enhancing operability of dividing wall column. *Industrial & Engineering Chemistry Research*, 56.
- Kaibel, G. (1987). Distillation columns with vertical partitions. *Chemical Engineering & Technology* 10, 1:92–98.
- Kister, H. Z. (1992). *Distillation design*. McGraw-Hill, New York.
- Kister, H. Z. and Gill, D. R. (1992). Flooding and pressure drop prediction for structured packings. 1:A109–A123.
- Kister, H. Z., Scherffius, J., Afshar, K., Abkar, E., and Corp, F. (2007). Realistically predict capacity and pressure drop for packed columns. 103.
- Korbelarova, J. (2017). Laboratory runs on kaibel column - process review. Technical report, Department of Chemical Engineering, Norwegian University of Science and Technology.
- Kvernland, M., Halvorsen, I. J., and Skogestad, S. (2010). Model predictive control of a Kaibel distillation column. In *Proceedings of the 9th International Symposium on DYCOPS 2010*, pages 539–544, Hoboken, NJ.
- Kvernland, M. K. (2009). *Model predictive control of a Kaibel distillation column, Master thesis*. Norwegian University of Science and Technology, Department of Engineering Cybernetics, Trondheim, Norway.
- Leva, M. (1954). Flow through irrigated dumped packings. *Chem. Eng. Progress Symp. Ser.*
- Lobo, W. E., Friend, L., Hashmall, F., and Zenz, F. (1945). Limiting capacity of dumped tower packings. *American Institute of Chemical Engineers – Transactions*, 41(6).
- Mackowiak, J. (2010). *Fluid Dynamics of Packed Columns*.
- Maćkowiak, J. (1991). Pressure drop in irrigated packed columns. *Chemical Engineering and Processing: Process Intensification*, 29(2):93 – 105.
- Maćkowiak, J. and Maćkowiak, J. F. (2014). Chapter 3 - random packings. In Górak, A. and Žarko Olujić, editors, *Distillation*, pages 85 – 144. Academic Press, Boston.

- Monro, D. (1938). Fractionating apparatus and method of fractionation.
- Olujčić, ., Jödecke, M., Shilkin, A., Schuch, G., and Kaibel, B. (2009). Equipment improvement trends in distillation. *Chemical Engineering and Processing: Process Intensification*, 48(6):1089 – 1104.
- Olujčić, Z. (1997). Development of a complete simulation model for predicting the hydraulic and separation performance of distillation columns equipped with structured packings. 11:31–46.
- Olujic, Z. (2016). Dividing wall column technology - recent developments and challenges. In *EFCE WP Fluid Separations*.
- Qian, X., Jia, S., Skogestad, S., and Yuan, X. (2016). Comparison of stabilizing control structures for dividing wall columns. *IFAC-PapersOnLine*, 49(7):729 – 734. 11th IFAC Symposium on Dynamics and Control of Process Systems Including Biosystems DYCOPS-CAB 2016.
- Rix, A. and Olujic, Z. (2008). Pressure drop of internals for packed columns. *Chemical Engineering and Processing: Process Intensification*, 47(9):1520 – 1529.
- Rocha, J. A., Bravo, J. L., and Fair, J. R. (1993). Distillation columns containing structured packings: a comprehensive model for their performance. 1. hydraulic models. *Industrial & Engineering Chemistry Research*, 32(4):641–651.
- Sherwood, T. K., Shipley, G. H., and Holloway, F. A. L. (1938). Flooding velocities in packed columns. *Industrial & Engineering Chemistry*, 30(7):765–769.
- Shilkin, A. and Kenig, E. Y. (2005). Fluid separation modelling in the columns equipped with structured packings using the hydrodynamic analogy. In Puigjaner, L. and Espuña, A., editors, *European Symposium on Computer-Aided Process Engineering-15, 38th European Symposium of the Working Party on Computer Aided Process Engineering*, volume 20 of *Computer Aided Chemical Engineering*, pages 331 – 336. Elsevier.
- Skogestad, S. (2003). Spurious activation of safety instrumented systems in the oil and gas industry: Basic concepts and formulas. *Journal of Process Control* 13, 4:291–309.
- Stichlmair, J., Bravo, J., and Fair, J. (1989). General model for prediction of pressure drop and capacity of countercurrent gas/liquid packed columns. *Gas Separation & Purification*, 3(1):19 – 28.

- Strandberg, J. (2011). *Optimal operation of dividing wall columns, Ph.D. thesis.* PhD thesis, Norwegian University of Science and Technology.
- Strandberg, J. and Skogestad, S. (2006). Stabilizing control of an integrated 4-product Kaibel column. In *Proceedings of IFAC International Symposium on Advanced Control of Chemical Processes (ADCHEM 2006), Gramado, Brazil 2*, pages 623–628.
- Strigle, R. F. (1994). *Packed tower design and applications: random and structured packings.* Gulf Pub. Co.
- Wolff, E. A. and Skogestad, S. (1995). Operation of integrated three-product (petlyuk) distillation columns. *Industrial & Engineering Chemistry Research*, 34(6):2094–2103.
- Wright, R. (1949). Fractionation apparatus.